energies

MDPI

Review

A Comprehensive Review on Advances in TiO_2 Nanotube (TNT)-Based Photocatalytic CO_2 Reduction to Value-Added Products

Md. Arif Hossen [1,2], H. M. Solayman [3], Kah Hon Leong [4], Lan Ching Sim [5], Nurashikin Yaacof [3], Azrina Abd Aziz [3,*], Wu Lihua [6] and Minhaj Uddin Monir [7]

1 Faculty of Chemical and Process Engineering Technology, Universiti Malaysia Pahang, Gambang 26300, Pahang, Malaysia
2 Center for Environmental Science & Engineering Research, Chittagong University of Engineering and Technology, Chattogram 4349, Bangladesh
3 Faculty of Civil Engineering Technology, Universiti Malaysia Pahang, Gambang 26300, Pahang, Malaysia
4 Department of Environmental Engineering, Faculty of Engineering and Green Technology, Universiti Tunku Abdul Rahman, Kampar 31900, Perak, Malaysia
5 Department of Chemical Engineering, Lee Kong Chian Faculty of Engineering and Science, Universiti Tunku Abdul Rahman, Kajang 43200, Selangor, Malaysia
6 Kuantan Sunny Scientific Collaboration Sdn. Bhd. Suites 7.23, 7th Floor, Imbi Plaza, Jalan Imbi, Kuala Lumpur 55100, Malaysia
7 Department of Petroleum and Mining Engineering, Jashore University of Science and Technology, Jashore 7408, Bangladesh
* Correspondence: azrinaaziz@ump.edu.my; Tel.: +60-103932711

Abstract: The photocatalytic reduction of CO_2 into solar fuels by using semiconductor photocatalysts is one of the most promising approaches in terms of pollution control as well as renewable energy sources. One of the crucial challenges for the 21st century is the development of potential photocatalysts and techniques to improve CO_2 photoreduction efficiency. TiO_2 nanotubes (TNTs) have recently attracted a great deal of research attention for their potential to convert CO_2 into useful compounds. Researchers are concentrating more on CO_2 reduction due to the rising trend in CO_2 emissions and are striving to improve the rate of CO_2 photoreduction by modifying TNTs with the appropriate configuration. In order to portray the potential applications of TNTs, it is imperative to critically evaluate recent developments in synthesis and modification methodologies and their capability to transform CO_2 into value-added chemicals. The current review provides an insightful understanding of TNT production methods, surface modification strategies used to enhance CO_2 photoreduction, and major findings from previous research, thereby revealing research gaps and upcoming challenges. Stability, reusability, and the improved performance of TNT photocatalysts under visible light as well as the selection of optimized modification methods are the identified barriers for CO_2 photoreduction into valuable products. Higher rates of efficacy and product yield can be attained by synthesizing suitable photocatalysts with addressing the limitations of TNTs and designing an optimized photoreactor in terms of the proper utilization of photocatalysts, incident lights, and the partial pressure of reactants.

Keywords: CO_2 photoreduction; synthesis; modification; photocatalyst; hydrocarbon fuels

Citation: Hossen, M.A.; Solayman, H.M.; Leong, K.H.; Sim, L.C.; Yaacof, N.; Abd Aziz, A.; Lihua, W.; Monir, M.U. A Comprehensive Review on Advances in TiO_2 Nanotube (TNT)-Based Photocatalytic CO_2 Reduction to Value-Added Products. *Energies* **2022**, *15*, 8751. https://doi.org/10.3390/en15228751

Academic Editor: Alan Brent

Received: 3 October 2022
Accepted: 16 November 2022
Published: 21 November 2022

1. Introduction

Development is required; however, it has to be conducted in a sustainable manner otherwise it will eventually pose a threat to humanity. In recent times, there has been a lot of focus on the imbalanced consequences of carbon dioxide (CO_2) on the ecosystem. In the overall atmospheric system, when the amount of CO_2 increases it creates a notable imbalance in the energy input into the planet, thereby leading to global temperature

rise [1,2]. It is widely known that rapid industrialization, exponential growth in the use of fossil fuels, and extensive deforestation are all contributing to a sharp rise in CO_2 emissions [3–5]. If current trends continue, CO_2 concentrations will reach 550 ppm by 2050, then a global temperature rise of +2 °C will be reached [3,6]. To mitigate the consequences of global warming, some strategies such as shifting to renewable energy sources, the effective use of energy as well as CO_2 reduction and utilization have to be considered.

Recently, various methods are being used for the conversion and utilization of CO_2. Artificial photosynthesis is a promising and trustworthy method for CO_2 reduction, and it is also a potential technique to achieve value-added compounds by using solar energy [7,8]. This is one of the most appealing alternatives, since it can both benefit from recycling atmospheric CO_2 with direct solar energy usage and meet the demand for renewable fuels [9,10]. TiO_2 has been extensively utilized as a photocatalyst in the photosynthesis process for CO_2 reduction due to its high photoactivity, excellent durability, affordability, and low toxicity [11,12]. Figure 1 depicts the general mechanism of the CO_2 photoreduction process when TiO_2 is used as a photocatalyst. However, practical applications of TiO_2 are greatly hindered by its wide inherent band gap (E_g = 3.2 eV for anatase), quick recombination of photogenerated charges, and low solar light utilization (about 5%) [13,14]. Therefore, the modification of TiO_2 is crucial for practical application.

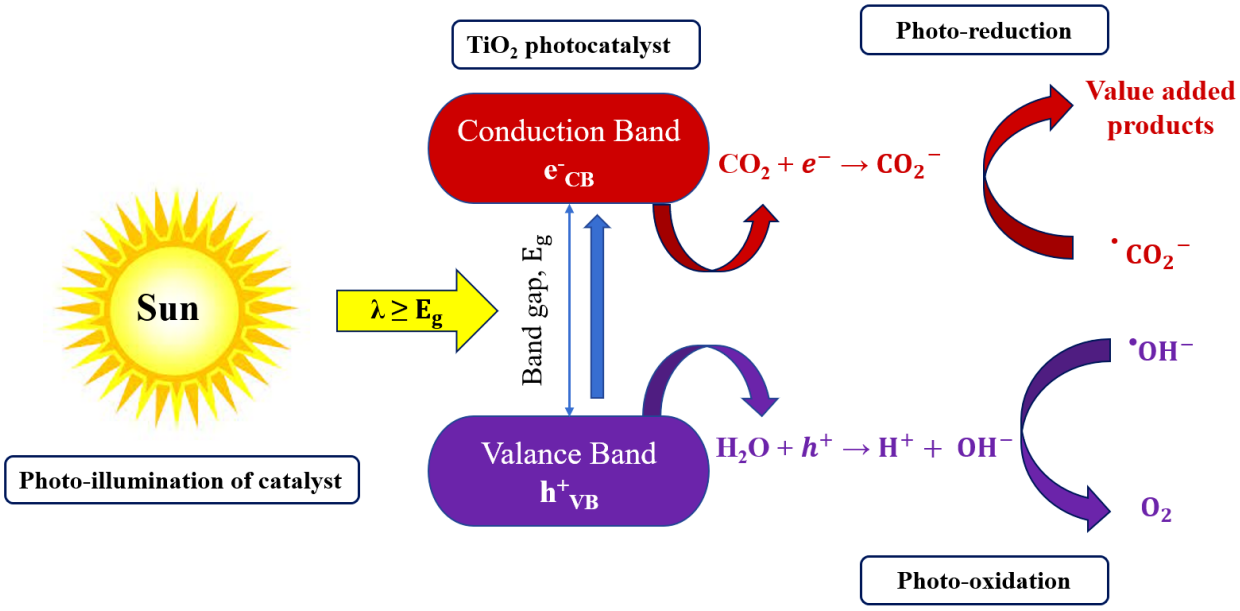

Figure 1. Schematic diagram of photocatalysis process of TiO_2-based photocatalysts for CO_2 reduction.

The photocatalytic performance of TiO_2 can be improved by modifying the surface of TiO_2. Due to their cost-effective construction, promising optical properties, and increased surface-to-volume ratio, TiO_2 nanotubes (TNTs) synthesized by electrochemical anodization have received special attention among the one-dimensional (1D) TiO_2 nanostructured materials [15,16]. In recent years, the use of TNTs for photocatalytic CO_2 reduction has grown tremendously, which can be visualized in Figure 2. Beginning in 2009, TNT photocatalysts have been used to reduce CO_2; since then, there has been a definite upward trend. Recently, remarkable studies are also going on to modify TNTs with different techniques such as doping, sensitization, and heterojunction for improving photocatalytic CO_2 reduction performance under visible light [17–21]. Therefore, a comprehensive overview of TNTs for applicability in reducing CO_2 is required along with new perspectives to facilitate potential directions for future research.

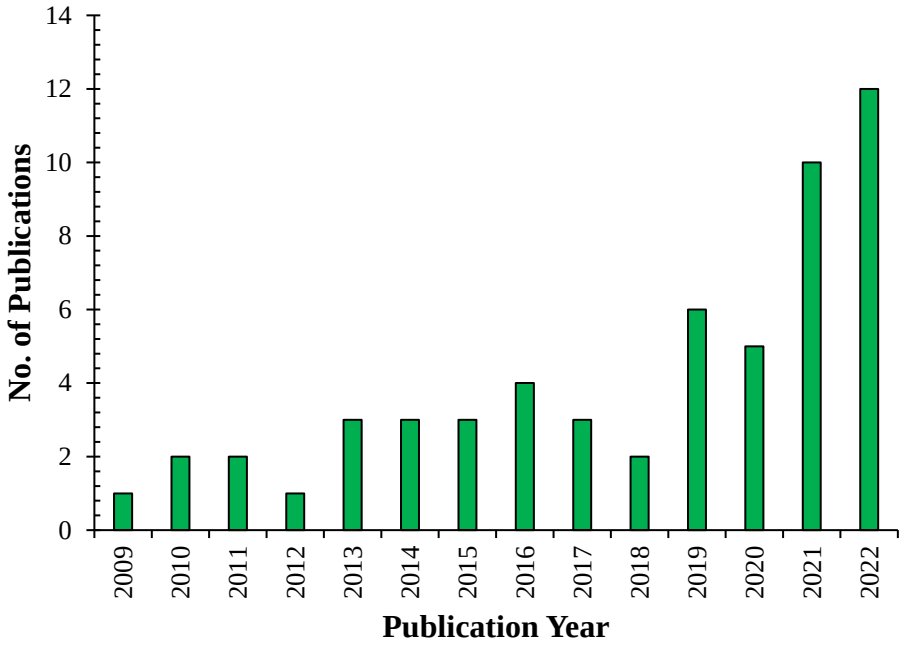

Figure 2. The number of publications using search string "TiO_2 nanotube and photocatalytic CO_2 reduction", (Scopus database search on 5 September 2022).

2. Scope and Overview of This Review

CO_2 is regarded as the most powerful and major contributor to global warming among other greenhouse gases. One of the most concerning environmental issues currently facing the world is CO_2 emissions [22,23]. To save the environment, it is indispensable to prevent the source of CO_2 emissions and at the same time convert CO_2 into valuable resources. In this connection, photocatalytic CO_2 reduction to value-added products is a promising approach. With the presence of substantial input energy to break down the C=O bond and suitable photocatalysts, CO_2 can be converted to value-added products such as hydrocarbons (CH_4, C_2H_4, C_2H_6) and oxygenated hydrocarbons (CH_3OH, C_2H_5OH, HCHO, HCOOH, CH_3COOH). During the photoreduction of CO_2, CO is generally observed as the most important intermediate product. Product selectivity is a very challenging task in the overall CO_2 photoreduction process [24,25]. Presently, plenty of research is going on using TiO_2-based photocatalysts to find suitable methods for enhancing the photocatalytic CO_2 reduction rate. Along with original research, some review works are also ongoing to portray the recent scenario to scientific bodies. Although there have been some reviews of photocatalytic CO_2 reduction using TiO_2 to produce CH_4 or other value-added chemicals, none of these reviews was entirely concerned with TNTs [6,26,27]. Consequently, in this review, we focused on photocatalytic CO_2 reduction to value-added products by employing TNTs. A comparative summary of previously reviewed articles on different structures and composites of TiO_2 for applications in diverse fields is presented in Table 1. Recent articles focusing on CO_2 photoreduction based on TNTs or modified TNTs are critically described. The authors believe that this comprehensive overview of the recent advances of TNT-based photocatalytic CO_2 reduction to value-added products would be useful to concerned researchers focusing on nanotechnology, materials science, chemical engineering, chemistry, and environmental science.

Table 1. Comparative summary of reviewed articles on different structures and composites of TiO_2 for variety of applications.

Review Type	Focused on	Application	Critically Reviewed	Reviewed Literature	Reference
Comprehensive	TiO_2 nanotubes	Photocatalytic CO_2 reduction to value-added products	Fabrication of TNTs, photocatalytic performance of TNTs, modification methods for improving CO_2 photoreduction activity under visible light and kinetics of CO_2 photoreduction	2010–2022	This study
Critical	TiO_2-based materials	Photocatalytic CO_2 reduction	Fundamentals and recent developments of TiO_2 photocatalyst, different modification techniques, future challenges for CO_2 photoreduction	2005–2017	[28]
Narrative	TiO_2-based nanostructures	Photocatalytic CO_2 conversion to valuable chemicals	Different structures of TiO_2, photocatalytic performance and their favorable reaction conditions	2008–2019	[29]
Narrative	TiO_2-based photocatalysts	Conversion of CO_2	Preparation and surface modification of TiO_2	1997–2018	[6]
Narrative	TiO_2 nanoparticles	H_2 production	Synthesis and characterization methods for doped-TiO_2; influence of dopants for improving photocatalytic performance of TiO_2	2005–2019	[30]
Narrative	TiO_2-based materials	Solar fuel production	Fabrication strategies and performance of visible light-responsive TiO_2-based materials for solar fuel production	2010–2020	[31]
Comprehensive review	TiO_2-based photocatalysts	H_2 fuel production	Key operating parameters affecting the photocatalytic performance of TiO_2-based photocatalysts	2002–2020	[26]
Narrative	TNTs	Dye-sensitized solar cells	Fabrication methods of TNT photoelectrode; modification of TNTs for enhancing power conversion efficiency	2001–2019	[32]
Narrative	TiO_2-based composites	Degradation of organic pollutants	Modification methods and performance of doped TiO_2-based photocatalysts	2008–2020	[33]
Narrative	TiO_2 nanorods	Applications as a photocatalyst and electrode	Synthesis and characterization of TiO_2 nanorods; mechanism and photocatalytic activity of TiO_2 nanorods	2005–2021	[34]
Narrative	Graphene coupled TiO_2 photocatalysts	Environmental applications	Fundamental mechanism, functionalization, and dynamics in TiO_2-graphene Nanocomposites	2000–2020	[35]
Perspective review	TiO_{2-x}-based materials	Photocatalytic CO_2 reduction	Recent progress in reduced TiO_2 catalysts for photocatalytic CO_2 reduction performance	2012–2022	[27]
Mini review	TiO_2-based Photocatalysts	Contaminant degradation	Different modification techniques; photocatalytic performance of TiO_2 for removal of emerging contaminants	2000–2021	[36]

3. Fundamentals of TNT

Titanium dioxide (TiO_2) or titania, has become a very recognized and highly studied photocatalyst in recent times due to its relatively long-term photostability, non-toxicity, availability, and photocatalytic activity [26,36]. In natural conditions, TiO_2 exists in four major crystal forms: anatase, rutile, brookite, and TiO_2(B). It is well documented in the literature that TiO_2 in the form of anatase has better photocatalytic performance than the rutile and brookite forms [35,37]. Among these forms, anatase is more advantageous for CO_2 photoreduction at the nanoscale due to its faster charge carrier separation, higher kinetic stability, lower surface energy, and acceptable bandgap energy [38,39]. The crystal structures of TiO_2 nanoparticles can be controlled by utilizing sugar alcohol such as D-sorbitol [40]. To improve the photocatalytic performance of pristine TiO_2, it is tuned to several shapes including 0D (nanoparticles), 1D (nanofibers, nanowires, nanorods, nanotubes), 2D (nanosheets, nanoflakes), and 3D (nanoflowers) (Figure 3). The nanotube shape has a larger surface area than other 1D forms of TiO_2 due to its additional inner walls. Both the inner and outer surfaces of TNTs are susceptible to modification. In addition, photons may have multiple reflections within the TNT hollow structure to facilitate its photocatalytic applications [41,42]. A longer diffusion length of materials leads to improved photoconversion efficiency, and this fact is widely acknowledged [43,44]. Lynch et al. [45] revealed that the electron diffusion length of nanotubes was roughly 30 times longer than that of other nanoparticles. Along with the morphology of the TNT photocatalyst, the composites' bonding strength also facilitates charge transfer [28]. TiO_2 nanotubes, having the advantages of relatively low toxicity, high chemical and thermal stability, high surface area, and reduced recombination rate, are known to be a desired photocatalyst for CO_2 photoreduction. Even though TNT has been utilized for CO_2 conversion to CH_4 and other value-added compounds, for improving photoreduction performance under visible light it is required to modify TNT.

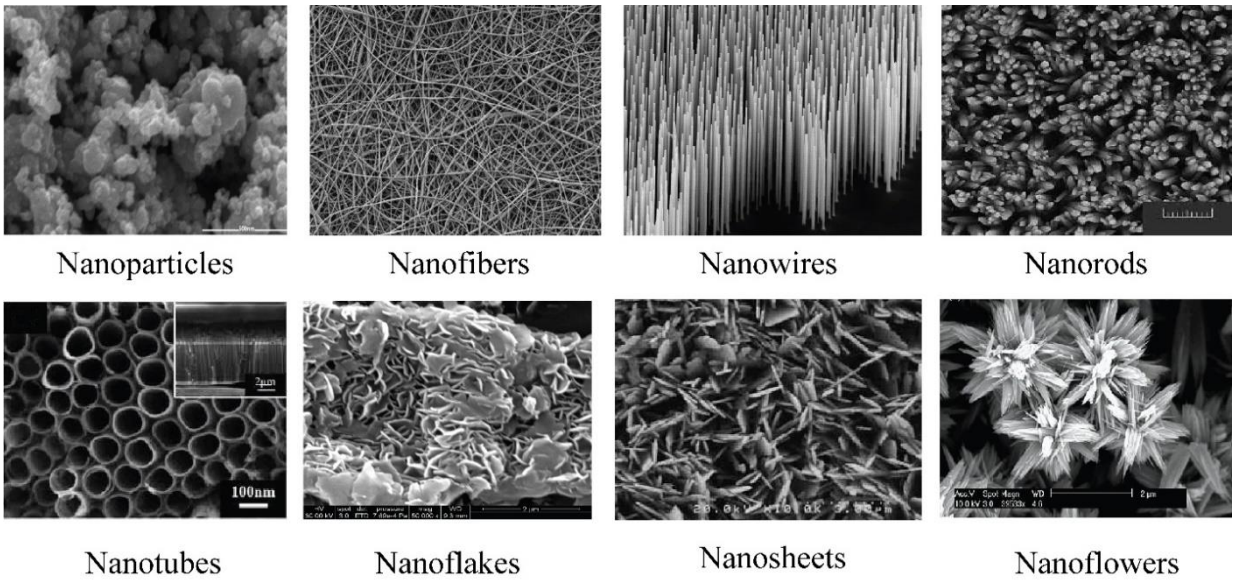

Figure 3. Different types of hierarchical nanostructures of TiO_2.

4. Synthesis of TNT

The one-dimensional (1D) tubular-structured TiO_2 nanotube (TNT) has received pervasive interest due to its unique structural morphology and wide range of applications [16]. TiO_2 nanotubes have a stronger catalytic performance than other 1D nanostructures in the activation- or diffusion-governed photocatalytic process due to their superior characteristics [39]. Sol-gel, template-assisted synthesis, hydrothermal treatment, and electrochemical anodization are frequently used methods for the synthesis of TNTs. The anodization

approach, among the other methods, allows for the development of self-organized TiO_2 nanotube arrays with the simplicity of geometry control (length, diameter, and wall thickness) by the use of appropriate anodization parameters [46]. The parameters that have a direct influence on the morphology of TNTs are electrolyte types, concentration, pH, temperature, anodization voltage, time, and type of electrodes [47,48]. The typical preparation of TNTs via the electrochemical anodization process is shown in Figure 4. The following steps are involved in TNTs' growing process: The initial oxide layer forms on a Ti substrate when a potential voltage is applied; the as-formed oxide layer is attacked by the Fluoride ions to produce TiF_6^{2-}, which will diffuse into the electrolyte; at the same time, oxidation continues to spread into the substrate; a relatively porous layer with a short anodization time is formed, and the interior of the layer dissolves as the anodization time increases, resulting in well-organized tubes with sufficient length and diameter.

The formation of TNTs by using sol-gel and hydrothermal methods is oriented randomly [49]. However, well-organized and vertically oriented TNTs with an average length can be achieved by electrochemical anodization, which enhances the charge transfer efficiency [50]. The anodization method is also preferable to the template assistant approach, in which the formation of nanotube morphology is limited by the used template geometry [43]. Hence, this method is widely utilized because of its controllable, strong adherent strength, achievability in tailoring the size and form of the NT arrays to the necessary dimensions, and capability to fulfill the requirements of specific applications.

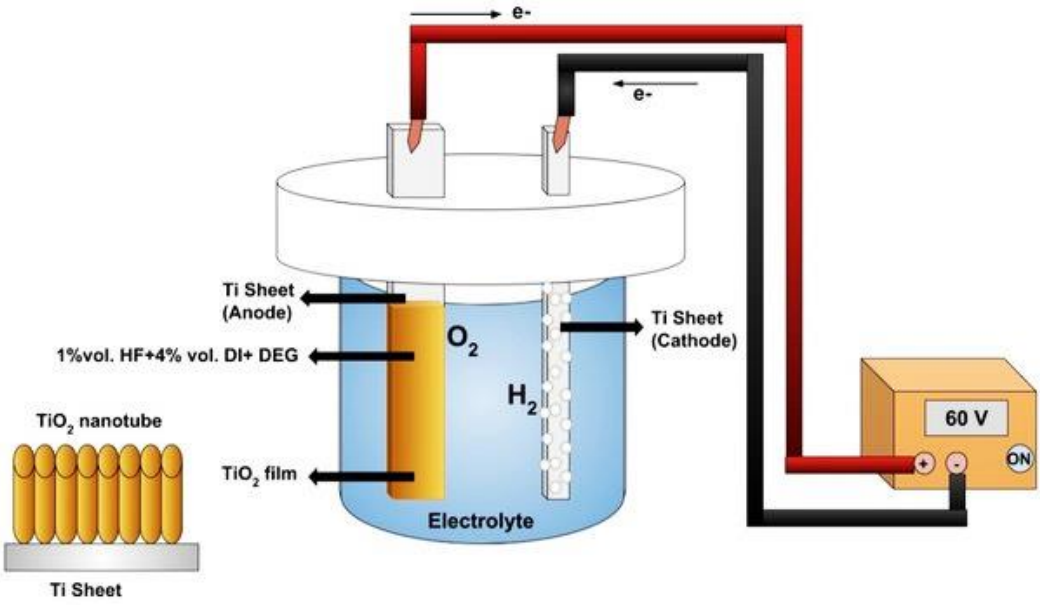

Figure 4. Illustration of electrochemical anodization process used to form TNTs, adopted from [51].

5. Basics about Photocatalytic CO_2 Reduction

Recently, a growing interest has been directed to conducting research in the field of photocatalytic CO_2 reduction, a novel technology for reducing CO_2 emissions while also producing renewable and sustainable fuels. However, CO_2 is a highly stable molecule (ΔG° = –400 kJ mol^{-1}) with linear symmetrical configuration, entirely oxidized carbon, and gross carbon-oxygen energy of up to 804.4 kJ mol^{-1} (at 298 K) [52]. As a result, it is not possible to convert it into value-added chemicals without the need for a photocatalyst or energy input. When exposed to photons with energy over the photocatalyst's band gap, the excited electrons (e^-) move from the valence band (VB) to the conduction band (CB), leaving empty holes (h^+) in the valence band. After that, some of the e^-/h^+ pairs go through rapid recombination and do not take part in the subsequent redox processes, which results in the loss of irradiation energy and conversion to some heat. The remaining electrons and holes move to the photocatalyst's surface to participate in reduction and

oxidation reactions. The photocatalytic reduction of CO_2 includes complex photocatalytic reaction mechanisms comprising proton-assisted multiple electron reduction steps with elevated energy barriers, low efficiency, activation and adsorption of CO_2 molecules, and product selectivity [53].

According to the literature, CO_2 photoreduction follows distinct chemical pathways depending on the reductant [54,55]. The formaldehyde and carbene pathways are the most widely acknowledged and confirmed CO_2 to CH_4 conversion processes, as shown in Figure 5. The first step in a reduction pathway is the formation of a $^{\bullet}CO_2^-$ anion radical by acquiring an electron from the CB of the photocatalyst. In the formaldehyde pathway, there are a number of possible intermediates in the conversion path of CO_2 to CH_4, which is indicated by blue arrows in Figure 5. The carbene pathway, which commences with deoxygenation followed by hydrogenation, is used to convert CO_2 to CH_4. The black arrows in Figure 5 illustrate the carbene pathway for CH_3OH/CH_4 production. There is still a lack of understanding regarding what happens during CO_2 photocatalysis. A thorough investigation of product selectivity is required to fully understand the mechanism of CO_2 reduction pathways [56,57].

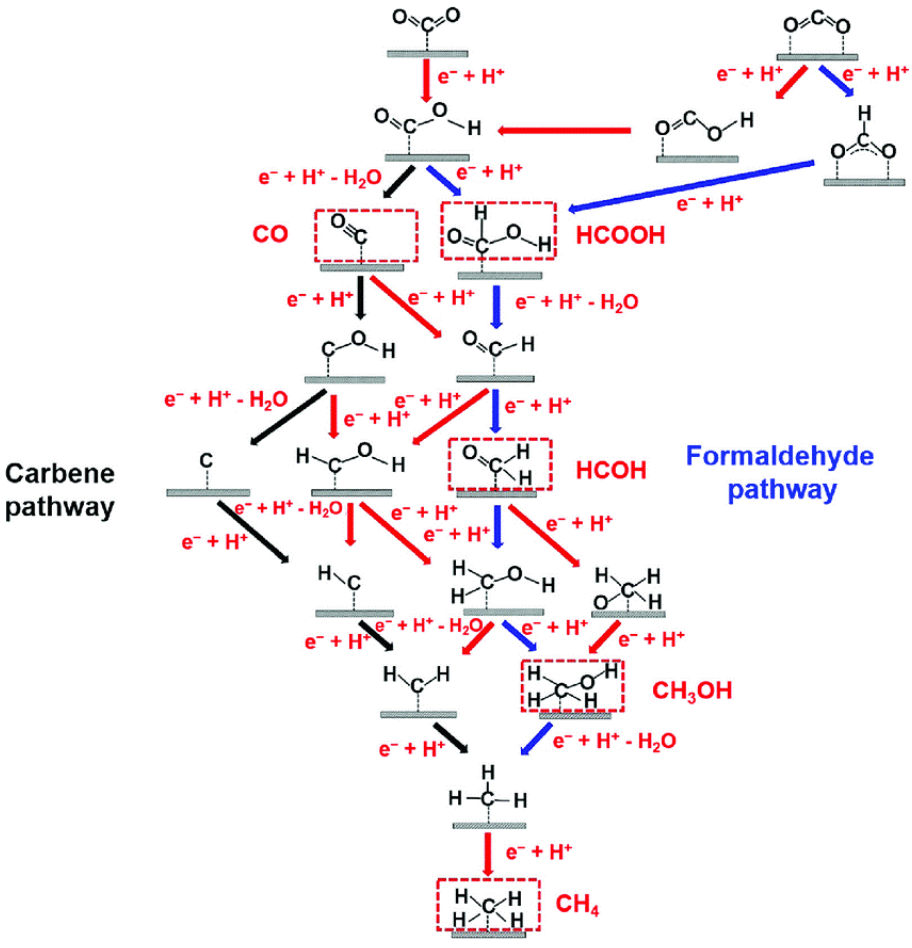

Figure 5. The possible pathways of photocatalytic CO_2 reduction to CH_4 or other hydrocarbon fuels on the surface of photocatalysts, retrieved from [56].

6. Photocatalytic CO_2 Reduction to Value-Added Products Solely Using TNT

TiO_2 in the configuration of nanotube arrays is highly desirable for practical application due to the morphological advantages that allow the most appealing diffusion of photocatalytic reduction products and a relatively low recombination rate [58]. The recent studies regarding photocatalytic performance for reducing CO_2 to hydrocarbon fuels using TNTs as a photocatalyst are summarized in Table 2. Depending on the length, diameter,

wall thickness, and crystal structure of the nanotubes the photocatalytic activity of TNT photocatalysts is greatly influenced. For instance, Savchuk et al. [59] found that the photocatalytic CO_2 reduction rate of multi-walled TNTs was 2-fold faster for CH_4 and 4-fold faster for CH_3OH production than single-walled TNTs. Oxygen vacancies and defects in the surface play a crucial role in enhancing the photoactivity of photocatalysts [60,61]. The photoactivity of synthesized black TiO_2 nanotube arrays (TNTA) was investigated by Gao et al. [62]. Black TNTA displayed excellent CO_2 photoreduction to CO, yielding 185.39 mol g^1 h^{-1} under irradiation of visible light. This was made possible by the oxygen vacancy self-doping, which significantly improved three important aspects, namely the development of photoinduced charge, transport of interfacial charge, and interfacial reaction.

Table 2. Photocatalytic performance of TNTs for CO_2 reduction.

Photocatalyst	Synthesis Method	Reactor	Reactant	Light Source	Product	Yield (μmol g^{-1} h^{-1})	Reference
Black TNTA	Electrochemical anodization	Gas-closed circulation system	CO_2 + H_2O	300 W Xe lamp	CO	185.4	[62]
Flame-annealed TNT	Electrochemical anodization	Stainless steel reactor with transparent quartz window	CO_2 + H_2O vapor	50 W LED lamp	CH_4	156.5	[63]
TNTA	Electrochemical anodization	Batch reactor with Fresnel lens and auto-tracking system	CO_2 + H_2O	Sunlight	CH_4 C_2H_4 C_2H_6	861.1 100.8 53.3	[64]
Amorphous TNTA	Electrochemical anodization	Three-way quartz reactor	CO_2 + H_2O	UV-light bulbs	CH_4	14.0	[65]
Self-doped TNT	Electrochemical anodization	Electric-assisted quartz reactor	CO_2 + H_2O vapor	UV LED lamp	CH_4 C_2H_6	682.3 52.6	[66]

Light intensity, reaction temperature, and the partial pressure of the reactant in the photocatalytic reactor have a significant impact on CO_2 photoreduction [67]. The photocatalytic performance of TiO_2 nanotube arrays (TNTA) under concentrated sunlight and different H_2O and CO_2 partial pressure was investigated by Zhang et al. [64]. The results exhibited that the photocatalytic performance of TNTA was 100 times greater than that of pure TiO_2 at 400 sunlight concentrated ratio and 0.05 MPa CO_2 pressure. For improving the performance of TNTs as a stand-alone photocatalyst different techniques have been used by researchers. When evaluating the photocatalytic CO_2 reduction, amorphous TNTA displayed promising photoactivity, providing a CH_4 generation rate of 14.0 without any modification methods [65]. Under visible light irradiation, flame-annealed TNTs synthesized in an aqueous electrolyte medium demonstrated superior photocatalytic performance and produced 156.5 μmol g^{-1} h^{-1} of CH_4 [63]. Pan et al. [66] established a unique electric-assisted photocatalytic method to lower the rate of electron and hole recombination. Using this technique, self-doped TNT photocatalyst was produced without using any electrolyte and counter electrode. Self-doped TNTs were able to convert CO_2 at maximum rates of 682.3 μmol g^{-1} h^{-1} for CH_4 and 52.6 μmol g^{-1} h^{-1} for C_2H_6, respectively. This indicates a 3.5-fold improvement in photocatalytic activity with the electric-assisted technique over conventional photocatalysis.

7. Modified TNT for Improving Photocatalytic Performance

To get over its well-known shortcomings of wide band gap and fast recombination rate, pure TiO_2 material typically undergoes various morphological and surface modifications. However, for improving the photoreduction activity of TNTs under visible light some modification methods are commonly used, as shown in Figure 6. Table 3 provides a summary of the benefits and limitations of the most adopted approaches for enhancing

the CO_2 photoreduction of the TNT-based photocatalysts. Details of different modification methods and the performance of modified TNTs are described in the following sections.

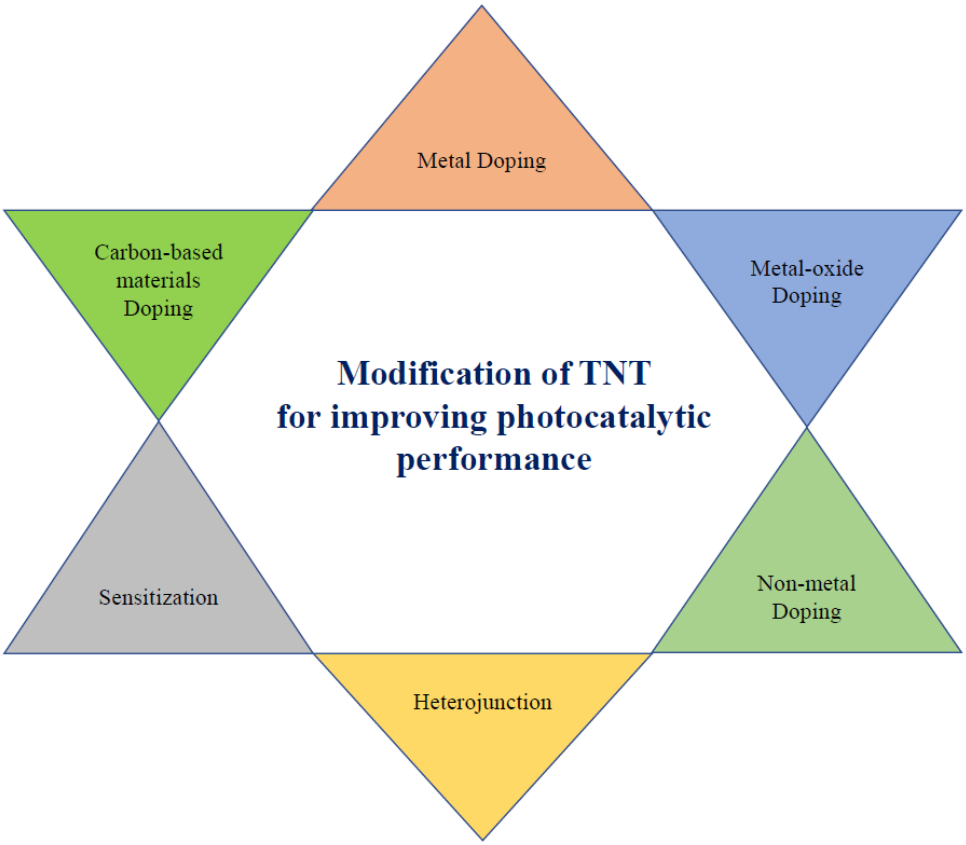

Figure 6. Modification methods used for improving the CO_2 photoreduction activity of TNTs.

Table 3. Comparison of various modification methods utilized for improving photocatalytic activity of TNTs.

Modification Methods	Criteria of Utilized Metals or Materials	Benefits	Limitations
Metal Doping	Transition metals	Effective method to expand the optical response of TiO_2-based nanocomposites.	Transition metals are expensive and rare as well as there is a possibility of metal leaching into the environment.
Metal-oxide Doping	Alkaline-earth metal oxides	Utilized to improve charge separation, light absorption, and structural properties.	Leads to structural defects.
Non-metal Doping	Mostly N and C	Narrow down the bandgap of TiO_2 by introducing new energy states.	Act as recombination centers.
Heterojunction	Semiconductor materials with narrow bandgap	Extends light absorption into visible range and separates reduction and oxidation sites.	This is complex approach with relatively lower stability.
Sensitization	Highly light-sensitive materials	Applied to improve the light response.	Development of photosensitized composite is challenging task.
Carbon-based Materials Doping	Chemically inert, nontoxic, and economically feasible	Extends light absorption into visible range, enhances electron–hole separation and improves CO_2 adsorption on catalytic surface.	Inhibits light absorption by TiO_2 materials.

7.1. Metal Doping

Metal doping is the most used technique to improve the photoreduction performance of TiO_2-based photocatalysts by introducing different energy levels under the CB and slowing down the fast recombination rate [68,69]. Transition metals, rare earth, and noble metals are the most reported metal dopants utilized to increase the photoactivity of TiO_2 [36,70–72]. For instance, Qian et al. [73] employed the transition metal niobium (Nb) with TNTA for enhancing CO_2 photoreduction under simulated solar irradiation. The results showed the production of CH_3CHO was over ~500 μmol g^{-1} h^{-1} with superior reusability and product selectivity. Nguyen et al. [74] examined molybdenum (Mo)-doped TNTs for enhancing CO_2 photoreduction. The incorporation of Mo substantially decreased the oxidation capability of TNTs, while improving photoreduction performance. Higher yields of CH_4 and CO have been reported for Mo-modified TNTs compared to bare TNTs. In another study, Ni and Cu metal was doped in TNT for exploring CO_2 photoreduction activity by Celaya et al. [18]. Doping Cu and Ni with TNT structures increased the density of the carriers, which enhances photoactivity, especially for Ni-doped TNT. In order to increase photoactivity, TiO_2 structures can also be altered using single-atom (SAs) catalysts, where all of the metals remain as isolated single atoms [75,76]. Single atom (SAs–Pt and Au) catalysts were deposited on TNTs by Pan et al. [77] for enhancing CO_2 photoreduction. The Pt-Au/R-TNTs with the addition of 0.33% of SA metals showed a 149-fold higher photocatalytic activity than untreated R-TNT, yielding CH_4 and C_2H_6 of 360.0 and 28.8 μmol g^{-1} h^{-1}, respectively. The quick shifting of photo-induced electrons from the defective sites to the SAs was made possible by the strong metal support interactions between Pt and Au. This also improved the separation of the electron holes and the transmission of the charge carriers.

With the aid of recent advances in plasmonic photocatalysis, the performance of CO_2 photoreduction under visible light exposure has rapidly increased [78]. It uses precious metal nanoparticles (NPs) spread over photocatalysts and has exceptional qualities including localized plasmonic surface resonance (LSPR), which helps to strengthen the absorption of visible light and excite active charge carriers [79]. The plasmonic effect is the consequence of the interaction between the incident beam of light and free electrons in metal nanoparticles. Additionally, plasmonic metal nanoparticles exhibit distinct optical, electrical, and thermal characteristics [80,81]. The most used plasmonic metals in metal doping with TiO_2 are gold (Au), silver (Ag), platinum (Pt), rhodium (Rh), and ruthenium (Ru) [82]. To enhance the yield of CH_4 through CO_2 photoreduction, Kar et al. [83] synthesized TNT arrays with Au and Ru nanoparticles. Under identical testing settings, the results showed that modified TNTAs produced CH_4 at a rate that was almost ten times greater than that of unmodified TNTAs. Low et al. [15], and Khatun et al. [84] investigated the photocatalytic performance of TNT arrays loaded with Ag and Au, respectively. In both cases, they found improved CO_2 photoreduction performance due to the LSPR behavior of the plasmonic metals.

7.2. Metal-Oxide Doping

A metal-oxide doping technique is also used to increase the photoactivity of pure TiO_2 due to their enhanced light absorption, charge separation, and surface chemistry [85,86]. Separation of charge is achieved at the junction of the metal oxide and TiO_2 material, resulting in a separation of redox processes that inhibits reactions from back and side and increases the production of the product from CO_2 photoreduction [11]. For instance, MgO/TNT films have been constructed by Li et al. [87] for investigating photocatalytic performance under visible light. They reported MgO/TNTs had excellent efficiency for the conversion of CO_2 to CH_4 compared with the TNTs alone due to MgO having a strong adsorption ability of CO_2.

Oxides of copper are the most active dopant compared with other metals used for improving the photoreduction performance of TiO_2 [11]. Shi et al. [88] used TNT-supported CuO-ZnO-CeO_2 (CZC) catalysts for enhancing the CO_2 hydrogenation to

CH_3OH. Figure 7a shows that among all catalysts, the catalyst (CZC) without TNT support exhibits the lowest CO_2 conversion. They asserted that adding TNT support to CZC catalysts enhanced CO_2 adsorption and increased the conversion of CO_2 to CH_3OH in addition to promoting CuO reducibility, improving metallic Cu dispersion, and increasing specific surface area. They also suggested a potential bifunctional CO_2 hydrogenation pathway over TNT-based CZC catalysts, as illustrated in Figure 7b. In another study, TNTs were modified with different ratios of Cu_2O/CuO for enhancing the CH_3OH yield from CO_2 photo-reduction [89]. When lactic acid was used as the electrolyte, TNT adjusted with an 80:20 CuO/Cu_2O ratio demonstrated the maximum CO_2 reduction performance. Recently, Goto et al. [90] examined the gas phase complex CO_2 photoreduction mechanism in high vacuum over Cu_2O-doped TNTAs. The positive synergistic effects of Cu_2O nanoparticles, and the appearance of TNA in the strong electron spin resonance signals, indicated the improvement of photoreduction. It is worth mentioning that although CO_2 deoxygenation to CH_4 is often the primary gas phase reaction, they found that CO_2 photoreduction happens by hydrogenation in the gas phase over Cu_2O-TNA photocatalysts even at high vacuum.

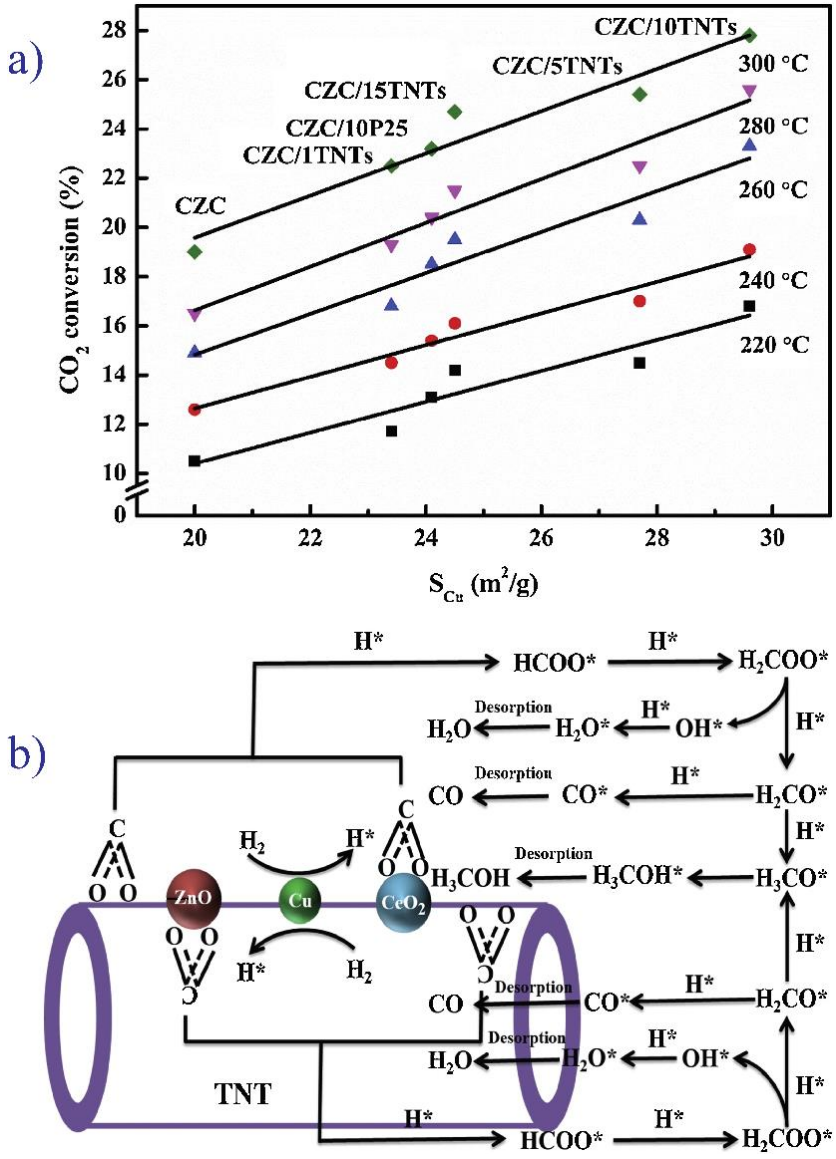

Figure 7. Role of TNT-supported CuO-ZnO-CeO_2 (CZC) catalyst: (**a**) CO_2 conversion rate versus Cu surface area (S_{Cu}) for various catalysts, and (**b**) possible bifunctional CO_2 hydrogenation mechanism for CH_3OH production, adopted from [88].

7.3. Non-Metal Doping

The photocatalytic activity of TiO_2 nanoparticles under the irradiation of visible light can be accelerated by non-metal doping. The deposition of dopants in the TiO_2 lattice may produce impurity states that impact the band gap, which controls important factors that influence the activity of photocatalysts, such as the charge transfer and recombination rate [91]. Although its usefulness is still controversial, doping with non-metallic anions, particularly nitrogen (N), has received a lot of attention in recent years [92]. For instance, Delavari et al. [93] synthesized N-doped TNT arrays for CO_2 photoreduction in the presence of CH_4. The results showed that the produced TNT arrays were highly organized, vertically aligned, and maintained their structural integrity after doping nitrogen. The photo-reduced products mostly consisted of H_2 with a selectivity of 80.5%, along with a number of additional by-products such as CO, C_2H_2, C_2H_4, and C_3H_8. Parayil et al. [94] examined nitrogen and carbon (C) doping with sodium TNT to enhance CO_2 photoconversion to hydrocarbon fuels. The N, C-TNT sample with a moderate doping concentration exhibited the highest CH_4 yield of 9.75 μmol g^{-1} h^{-1}. Light absorption, specific surface area, and the concentration of Na^+ ions in TNT, which act as CO_2 adsorption sites and center the photogenerated electrons, were the main parameters that improved the performance of the modified photocatalyst.

7.4. Heterojunction

The heterojunction technique is becoming a very promising approach for the control of the charge recombination rate as well as for achieving optimal conduction band (CB) and valance band (VB) edge positions for improved photocatalytic activity [95,96]. In particular, the Z-scheme method encourages strong redox facilities that are helpful for the production and propagation of electron holes [97]. The challenge in CO_2 reduction is the appropriate fabrication of Z-scheme between TiO_2 and other semiconductors with higher CB potential. Lai et al. [98] successfully synthesized ZnO–Au-TNT Z-scheme heterojunction with a CH_3OH yield of 7.78 mmol g^{-1} h^{-1} for CO_2 reduction. In another study, Wu et al. [99] investigated the CO_2 photoreduction performance of P–O-linked g-C_3N_4-TNT Z-scheme composites. The synergistic effect between g-C_3N_4 and P–O links plays a crucial role in the modified Z-scheme heterostructure and showed a more than 3-fold higher CO_2 photoreduction than bare TNTs. The schematic diagram of the charge transfer and separation mechanism of the structured Z-scheme P–O-connected g-C_3N_4-TNTs is shown in Figure 8. When both TNTs and g-C_3N_4 were excited appropriately, the photogenerated electrons on the CB of the TNTs interact with the holes on the VB of g-C_3N_4. As a result, the energy-rich holes left on the VB of the TNTs and the electrons left on the CB of g-C_3N_4 participate in redox processes, promoting charge separation and enhancing CO_2 photoreduction. The photoreduction performance of the g-C_3N_4-rGO-TNT heterostructure was also examined by Ikreedeegh and Tahir [100]. Using an optimized g-C_3N_4-rGO-TNT combination after 4 h irradiation, they found elevated CH_4 and CO production of 3.32 and 47.12 mmol m^{-2}, respectively, which represents a significant improvement compared to pristine TNTs.

A TNT photocatalyst synthesized by the hydrothermal method was modified to a CdS(or Bi_2S_3)/TNT heterostructure by Li et al. [101] for enhancing photocatalytic CO_2 reduction activity under the visible spectrum of light. The maximum production of CH_3OH, which was almost 2.2 times more than that of bare TNTs, was achieved on a modified Bi_2S_3/TNT photocatalyst. Kim et al. [19] constructed a TNT-$ZnIn_2S_4$ type II heterojunction by a simple hydrothermal approach for highly selective CO_2 photoreduction. The results showed a significant improvement with a 4.41 mmol g^{-1} h^{-1} yield of CO, which was 1.5 times higher than bare TNTs. The TNT-$ZnIn_2S_4$ composite extends the responsive spectral range and accelerates the separation of photoexcited electrons during CO_2 conversion.

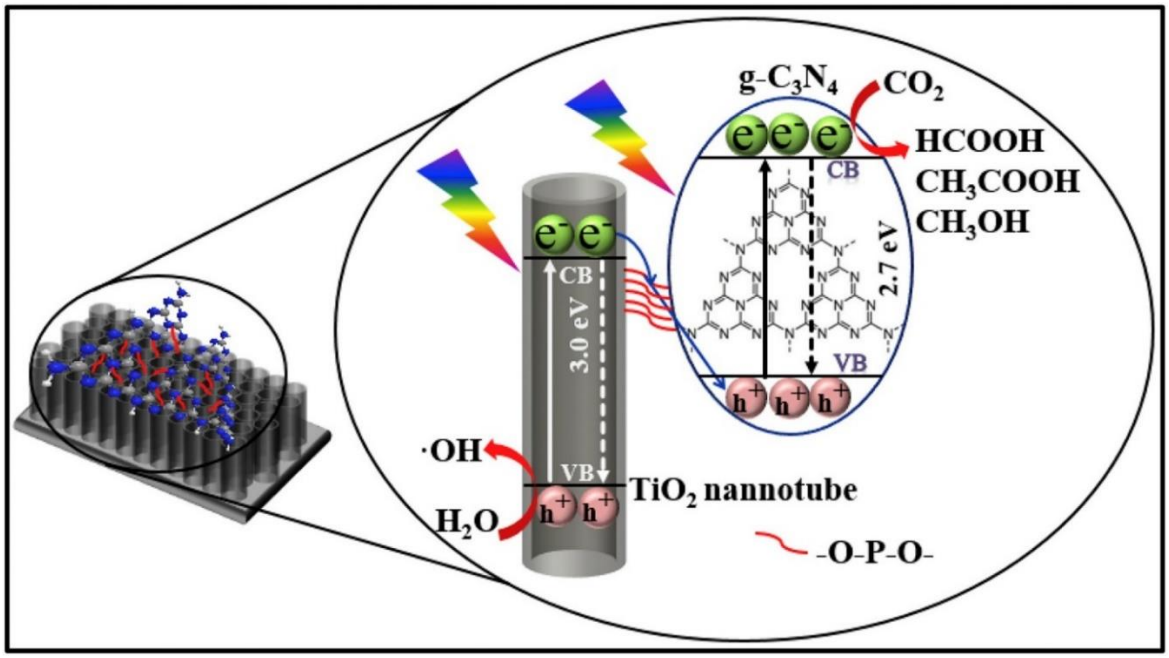

Figure 8. Schematic representation of photogenerated charge transfer and separation mechanism of the built P–O-connected g-C_3N_4-TNT composites, adopted from [99].

7.5. Sensitization

The wavelength of light can be expanded by surface photosensitization, which also improves the performance of the excitation process [96]. By utilizing sensitizers, the rate of visible light absorption can also be increased. This approach has been utilized in various studies for CO_2 photoreduction. For instance, Cheng et al. [102] incorporated CdS/ZnS quantum dots as a sensitizer with TNT arrays for enhancing the CO_2 conversion rate under the illumination of visible light. Before the incorporation of sensitizer, the photocatalytic conversion efficiency of TNTA under visible light was too low. Results showed a 2.73 times improvement in CH_3OH yield after sensitizing TNTA with CdS/ZnS quantum dots. Xiao et al. [20,21] successfully synthesized Ni(II) tetra(4-carboxylphenyl)porphyrin (NiTCP) and cobalt tetra(4-carboxyphenyl)porphyrin (CoTCP) with TNT arrays for efficient CO_2 photoreduction to CH_4. Under visible light sources, CoTCP-TNTAs produced 5.5 times more CH_4 than bare TNT arrays, while NiTCP-TNTAs produced 5 times higher CH_4. The photoexcitation of electrons occurs from the highest occupied molecular orbital (HOMO) of the sensitizer to its lowest unoccupied molecular orbital (LUMO). As depicted in Figure 9, photogenerated electrons are transferred from the LUMO of the sensitizer to the CB of the TiO_2, where they are then consumed by the CO_2 reactant.

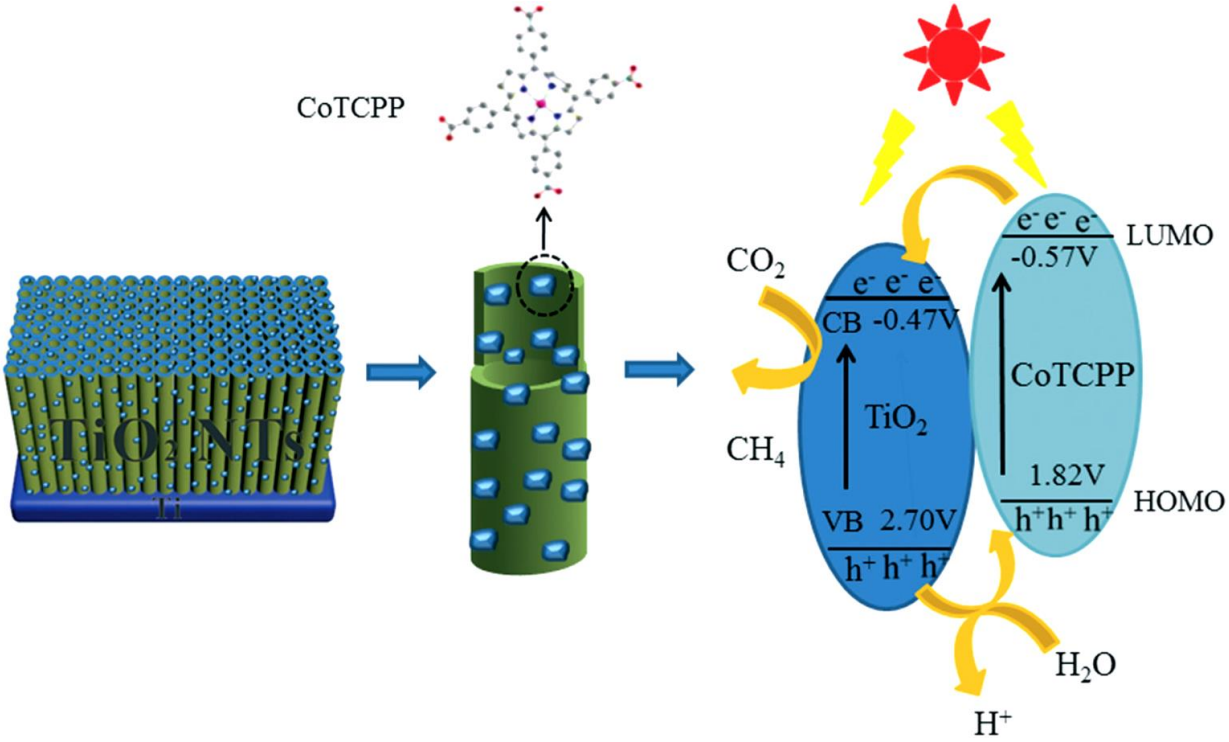

Figure 9. Schematic diagram of possible mechanism for CO_2 photoreduction over sensitized TNT arrays, adopted from [21].

7.6. Carbon-Based Material Doping

Carbon-based nanostructures such as carbon quantum dots (CQDs), graphene quantum dots (GQDs), carbon nanotubes (CNT), graphene oxide (GO), and reduced graphene oxide (rGO) are often used to enhance the photoactivity of TiO_2-based photocatalysts [103]. Due to strong photoluminescence, high electrical conductivity, wide solar absorption spectrum, and affordable cost, carbon-based materials have drawn the greatest attention to be used as a co-catalyst in enhancing photoactivity [17,104]. To increase CO_2 photoreduction performance under visible light, GO and rGO were used with TNTs as co-catalyst as presented in Table 2. Under visible light irradiation, the graphene oxide (GO) layer links the NTs on their surface, which helps to enhance the mobility of the electrons [105]. The combination of the carbon-based materials along with TNTs acts as a strong photocatalyst to improve CO_2 photoreduction [17,106]. A possible synergetic mechanism to enhance the CO_2 photoreduction over the CQD-modified TNTs is shown in Figure 10. The following are some major ways that CQDs contribute to the improvement of CO_2 photoreduction. The electrons in the CB of the TNTs are transferred to CQDs during the photocatalytic process and quickly react with CO_2, which prevents charge recombination; in the composite long-wavelength visible light is absorbed and converted to short-wavelength by CQDs, which then excites TNTs to increase charge separation; and in the third case, the CQDs serve as a reservoir to trap electrons emitted from TNTs, which prevents charge recombination [17].

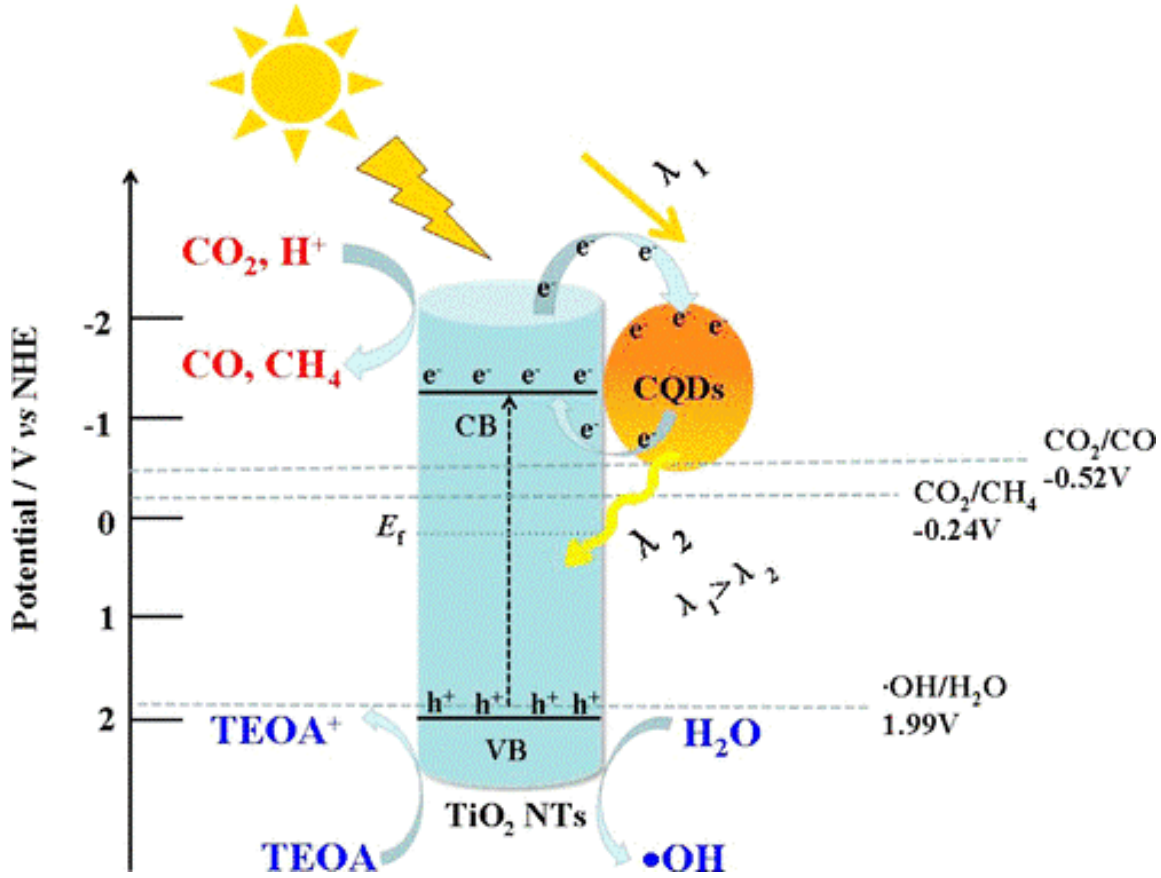

Figure 10. Photocatalytic CO_2 reduction mechanism over CQD-modified TNTs, retrieved from [17].

As shown in Table 4, substantial improvements have been noticed converting CO_2 into solar fuels when utilizing carbon-based materials as a co-catalyst with TNT. The maximum rate of CO_2 conversion to produce CH_4 was reported by Zubair et al. [107] with the use of GQDs. It has been documented that the mobility of photogenerated charge carriers between the GQDs and TNT crystals plays a crucial role in the photocatalytic performance of the attained composites. A considerable improvement in the production of CH_4 has also been noticed with TNT arrays modified by rGO.

Table 4. Summary of carbon-based material-doped TNT photocatalysts used for CO_2 photoreduction.

Composite Photocatalysts	TNT Fabrication Method	Photoreactor	Light Source	Product	% of Yield Increased than TNT	Reference
CQDs-TNTs	Hydrothermal method	Electrochemical workstation	300 W Xe lamp	CO CH_4	2.4 2.5	[17]
TNT-rGO-Pt	Electrochemical anodization	Circular stainless steel batch reactor	400 W metal-halide lamp	CH_4	2.8	[105]
GQD-TNTA	Anodization	Stainless steel reactor	100 W Xe lamp	CH_4	5.6	[107]
rGO-Pt-TNTA	Anodization	Gas–solid phase photoreactor	500 W tungsten–halogen lamp	CH_4	1.9	[108]
rGO-TNTA	Electrochemical anodization	Stainless steel cell	100 W Xe light	CH_4	4.4	[109]
GO-TNT	Electrochemical anodization	Cylindrical quartz reactor	200 W UV-A lamp	CO	2.3	[110]

8. Kinetic Modeling to Compute Rate of CO_2 Photoreduction

There is a very limited number of studies focusing on the kinetic model of CO_2 photoreduction. An intrinsic model is highly useful, since it avoids scale dependency and it explains the kinetics of the entire process where all active sites on the photocatalyst surface have an equal possibility to participate in the reaction [111]. Empirical modeling, in situ analysis, and microkinetic approaches are generally used for computing the rate of CO_2 photoreduction [112]. In heterogeneous photocatalysis, the kinetic models are utilized for the well-stable reactants and products in terms of the concentrations of reactant and product on the surface of photocatalysts. In general, the constants of reaction rate and adsorption equilibrium are chosen as kinetic parameters.

There are five key steps that generally occur within the photocatalytic reactor as shown in Figure 11. Step 1 is the initiation of reactants to the reactor, i.e., the diffusion of H_2O and CO_2 to the photocatalyst's surface; step 2 consists of diffusion along the surface-active sites; step 3 is the provision of the energy for the reaction; step 4 consists of the photoreaction between the two adjacent active sites; while step 5 belongs to the desorption of products from the surface of the photocatalyst [111]. The most crucial factors influencing photocatalytic reduction efficiency are the interactions between the CO_2 molecules and the photocatalyst surfaces. Computational modeling employing density function theory (DFT) simulations has been applied to investigate the CO_2 photoreduction processes occurring at the surface of TiO_2 photocatalysts by Liu et al. [113], and Núñez et al. [114]. Computational fluid dynamics and the Sips model were used by Khalilzadeh and Shariati [115], and Lu et al. [116] to investigate the CO_2 photoreduction rate over TiO_2 photocatalysts. So far, no study regarding computational modeling has been conducted on TNT photocatalysts. When evaluating the assumptions established for empirical kinetic studies, it is also vital to understand the molecular processes appearing at the surface of the photocatalyst. The use of in situ analysis methods is a more promising way to study the CO_2 photoreduction activities appearing on the surface of photocatalysts [111]. Photoluminescence (PL), Fourier Transform Raman Infrared Spectroscopy (FTIR), and X-ray photoelectron spectroscopy (XPS) are examples of in situ spectroscopy that provide vital information on the CO_2 photoreduction process. A kinetic study of CO_2 photoreduction over TNTs using in situ FTIR, UV–vis, and X-ray absorption spectroscopies, has been reported by Liu et al. [113], and Chang et al. [42]. Their findings provided evidence that carboxylate species adsorbed on TNT might carry out surface reactions that are accelerated by UV-vis light to produce low-carbon compounds.

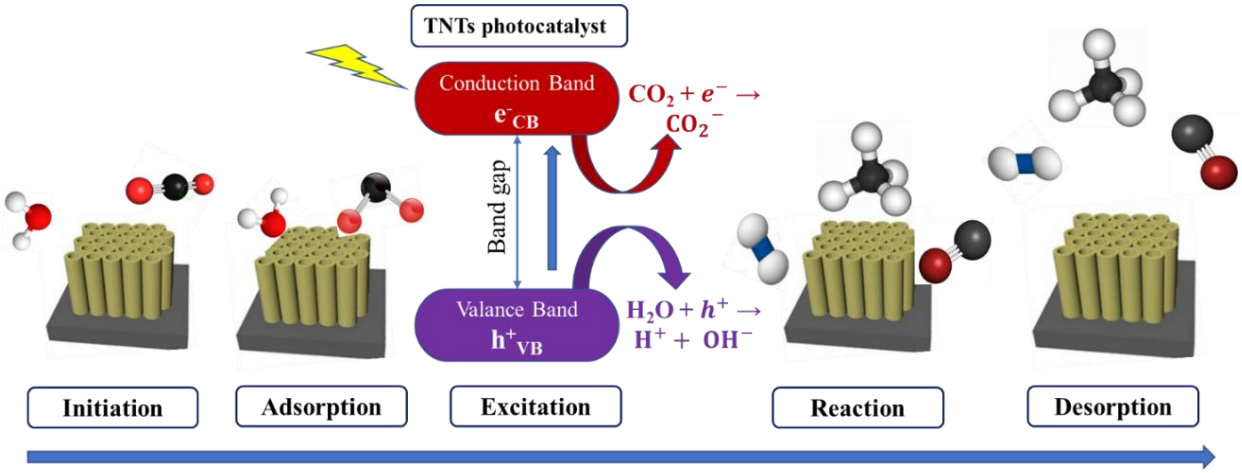

Figure 11. Possible steps occurring in photoreactor for CO_2 photoreduction.

Microkinetics is the study of the fundamental processes taking place at a molecular level on the surface of photocatalysts without taking into account the effects of heat and mass transfer [117]. Microkinetic analysis is a viable technique for propelling CO_2 photore-

duction forward. A benefit of employing this technique is that it saves time and money in the lab by producing models that can be used to screen and direct photocatalyst design [114]. The development of scientifically justified Langmuir–Hinshelwood (LH)-based kinetic models provides an alternative approach to microkinetic modeling. This type of model was previously used by Bjelajac et al. [118], and Tan et al. [119] to illustrate the kinetics of TiO_2-based CO_2 photoreduction. The benefit of this method is its simplicity, and it takes into account the effects of partial pressure as well as irradiation on the kinetic data. The time and effort necessary to acquire CO_2 photoreduction kinetic data are a drawback. Reaction rates in non-homogeneous photocatalytic approaches are typically related to the effective desorption of the end products on the photocatalyst surface after reactant adsorption [119,120]. The reaction rate is an indicator of photocatalytic activity represented as the number of moles that have reacted in a given amount of time and space, as evaluated by this approach. The typical assumption is that the surface reactions are the slowest and ultimately the rate-determining step. The L–H mechanism can be utilized for such reactions if indeed the reactants are effectively adsorbed within the same adsorbent surface with distinct rate constants. When CO_2 and H_2O are employed as reactants, and it is assumed that they are adsorbed on the identical active sites just on the catalyst surface, the L–H model can be used to compute the rate of reaction as illustrated in Equation (1).

$$\text{Rate} = (\text{kI}^{\alpha}) \left[\frac{K_{CO_2} P_{CO_2} K_{H_2O} P_{H_2O}}{\left(1 + K_{CO_2} P_{CO_2} + K_{H_2O} P_{H_2O} + K_{CH_4} P_{CH_4} + K_{CO} P_{CO} + K_{H_2} P_{H_2}\right)^2}\right] \quad (1)$$

Here, k stands for the rate constant of any specific product, and I is the amount of incident light that is used to calculate the kinetic constants. Generally, the rate of a photocatalytic reaction is proportional to I^{α}, where α denotes the reaction order of light intensity and depending on the intensity of light its value never exceeds one. K_{CO_2}, K_{H_2O}, K_{CH_4}, K_{CO}, and K_{H_2} are the ratios of rate constants for the adsorption and desorption of CO_2, H_2O, CH_4, CO, and H_2, respectively. If only reactants are adsorbed on the surface of the photocatalysts and all products are instantly desorbed following chemical reaction, Equation (1) can be simplified. The simplified form of the L–H model will be as Equation (2).

$$\text{Rate} = (\text{kI}^{\alpha}) \left[\frac{K_{CO_2} P_{CO_2} K_{H_2O} P_{H_2O}}{\left(1 + K_{CO_2} P_{CO_2} + K_{H_2O} P_{H_2O}\right)^2}\right] \quad (2)$$

By comparing it to the experimental data of P_{CO_2}, P_{H_2O}, light intensity, and the rate of hydrocarbon production, the constants of the L–H model can be resolved. Delavari et al. [84] used the L–H model for investigating the CO_2 photoreduction rate over N-doped TNTA. It has been observed that when only a small portion of the sites is utilized the reaction rate is entirely proportional to P_{CO_2} at a lower partial pressure. However, with the increase in P_{CO_2}, the rate eventually slows down and becomes less reliant on it, probably because of CO_2 adsorption on the whole surface of the photocatalyst. Moreover, the rate of reaction is slowed down since CH_4 molecules must compete with CO_2 molecules to commence chemical reactions.

The catalyst surface is frequently employed as a reaction space in heterogeneous catalytic processes [121]. The participation of light in the initiation of certain catalytic processes adds some complexity to photocatalysis. The reaction space cannot be described by only one single parameter because both the quantity of the photocatalyst and the light are essential to measure the rate of reaction at a specific position in the reaction space. The Kinetic Monte Carlo (KMC) simulation model is rapidly becoming the benchmark for bridging the gap between the large diversity of length scales and time scales across which heterogeneous catalysis unfolds [122]. In a nutshell, the kinetics of CO_2 photoreduction are greatly influenced by the source of light, temperature, and pressure in the photoreactor [111]. In both gas and liquid phase systems, partial pressure influences the

possibility of adsorption over the photocatalyst, increasing the yield of the photocatalytic CO_2 reduction [28].

9. Concluding Remarks and Future Perspective

TiO_2 nanotubes are promising photocatalysts that have been utilized for CO_2 photoreduction to harvest solar fuels. TiO_2 nanotubes can be produced in a wide range of morphologies utilizing a simple electrochemical anodization process. This review critically assesses the advancement of TNT application on CO_2 photoreduction over the last ten years. The detailed description of kinetic approaches to compute the rate of CO_2 photoreduction has also been summarized in this study. Overall, notable progress has been made in the reduction of CO_2 using bare TNTs or modified TNTs. TiO_2 nanotube photocatalysts utilized by raising the incident light intensity and reaction temperature by using concentrated sunlight have been shown to achieve excellent CO_2 photoreduction to CH_4. In the case of modified TNTs, ZnO–Au–TNT Z-scheme heterojunction showed the maximum CO_2 reduction with a CH_3OH yield of 7.78 mmol g^{-1} h^{-1}. Among the carbon-based materials, GQD-modified TNTs showed 5.6 times higher CO_2 photoreduction performance than pristine TNTs. Langmuir–Hinshelwood (LH) is the most utilized model to compute the rate of reaction during photocatalytic CO_2 reduction to value-added products.

Despite extensive research in this area, the photocatalytic reduction of CO_2 is still far from practical application due to the low yield of products. Studies have been undertaken so far on a lab scale, and there is still a long way to go before the technologies are taken into consideration for large-scale applications. The control of charge-carrier recombination, performance under visible light, quick charge separation, peeling off TNTs from substrate along with the utilization of the whole surface of the photocatalyst in a photoreactor, and cost-effective and environmentally friendly surface modification methods are all issues that need to be addressed for improving the performance of TNT photocatalysts. The stability and reusability of photocatalysts as well as cost-efficiency and more comprehensive kinetic modeling are crucial for scaling up the CO_2 photoreduction process. However, these have been rarely addressed in previous studies. More research is required on the cost-effective and reusable photocatalyst synthesis method, photoreactor design, kinetic modeling, and pilot-scale implementation.

Author Contributions: Conceptualization, methodology, writing—review and editing, M.A.H. and W.L.; supervision, A.A.A. and N.Y.; writing—review and editing, K.H.L., M.U.M., H.M.S. and L.C.S. All authors have read and agreed to the published version of the manuscript.

Funding: This research supported by the Universiti Malaysia Pahang (UMP) internal grant, Product Development Unit Grant (PDU 213221).

Data Availability Statement: Data can be available on requesting the corresponding author and first author.

Acknowledgments: This study was supported by the Universiti Malaysia Pahang (UMP) internal grant, Product Development Unit Grant (PDU 213221). The authors express gratitude for the grant.

Conflicts of Interest: The authors declare no conflict of interest.

References

1. Derichter, R.K.; Ming, T.; Caillol, S. Fighting global warming by photocatalytic reduction of CO_2 using giant photocatalytic reactors. *Renew. Sustain. Energy Rev.* **2013**, *19*, 82–106. [CrossRef]
2. Rahman, F.A.; Aziz, M.M.A.; Saidur, R.; Bakar, W.A.W.A.; Hainin, M.R.; Putrajaya, R.; Hassan, N.A. Pollution to solution: Capture and sequestration of carbon dioxide (CO_2) and its utilization as a renewable energy source for a sustainable future. *Renew. Sustain. Energy Rev.* **2017**, *71*, 112–126. [CrossRef]
3. Ahmed, S.; Ahmed, K.; Ismail, M. Predictive analysis of CO_2 emissions and the role of environmental technology, energy use and economic output: Evidence from emerging economies. *Air Qual. Atmos. Health* **2020**, *13*, 1035–1044. [CrossRef]
4. Sun, Y.; Hao, Q.; Cui, C.; Shan, Y.; Zhao, W.; Wang, D.; Zhang, Z.; Guan, D. Emission accounting and drivers in East African countries. *Appl. Energy* **2022**, *312*, 118805. [CrossRef]

5. de Brito, J.F.; Bessegato, G.G.; Perini, J.A.L.; de Moura Torquato, L.D.; Zanoni, M.V.B. Advances in photoelectroreduction of CO_2 to hydrocarbons fuels: Contributions of functional materials. *J. CO2 Util.* **2022**, *55*, 101810. [CrossRef]
6. Al Jitan, S.; Palmisano, G.; Garlisi, C. Synthesis and surface modification of TiO_2-based photocatalysts for the conversion of CO_2. *Catalysts* **2020**, *10*, 277. [CrossRef]
7. Smith, P.T.; Nichols, E.M.; Cao, Z.; Chang, C.J. Hybrid Catalysts for Artificial Photosynthesis: Merging Approaches from Molecular, Materials, and Biological Catalysis. *Acc. Chem. Res.* **2020**, *53*, 575–587. [CrossRef] [PubMed]
8. Ezugwu, C.I.; Liu, S.; Li, C.; Zhuiykov, S.; Roy, S.; Verpoort, F. Engineering metal-organic frameworks for efficient photocatalytic conversion of CO_2 into solar fuels. *Coord. Chem. Rev.* **2022**, *450*, 214245. [CrossRef]
9. Hou, H.; Zhang, X. Rational design of 1D/2D heterostructured photocatalyst for energy and environmental applications. *Chem. Eng. J.* **2020**, *395*, 125030. [CrossRef]
10. Albero, J.; Peng, Y.; García, H. Photocatalytic CO_2 Reduction to C2+ Products. *ACS Catal.* **2020**, *10*, 5734–5749. [CrossRef]
11. Adekoya, D.; Tahir, M.; Amin, N.A.S. Recent trends in photocatalytic materials for reduction of carbon dioxide to methanol. *Renew. Sustain. Energy Rev.* **2019**, *116*, 109389. [CrossRef]
12. He, X.; Wu, M.; Ao, Z.; Lai, B.; Zhou, Y.; An, T.; Wang, S. Metal–organic frameworks derived C/TiO_2 for visible light photocatalysis: Simple synthesis and contribution of carbon species. *J. Hazard. Mater.* **2021**, *403*, 124048. [CrossRef] [PubMed]
13. Shtyka, O.; Shatsila, V.; Ciesielski, R.; Kedziora, A.; Maniukiewicz, W.; Dubkov, S.; Gromov, D.; Tarasov, A.; Rogowski, J.; Stadnichenko, A.; et al. Adsorption and photocatalytic reduction of carbon dioxide on TiO_2. *Catalysts* **2021**, *11*, 47. [CrossRef]
14. Zu, M.; Zhou, X.; Zhang, S.; Qian, S.; Li, D.S.; Liu, X.; Zhang, S. Sustainable engineering of TiO_2-based advanced oxidation technologies: From photocatalyst to application devices. *J. Mater. Sci. Technol.* **2021**, *78*, 202–222. [CrossRef]
15. Low, J.; Qiu, S.; Xu, D.; Jiang, C.; Cheng, B. Direct evidence and enhancement of surface plasmon resonance effect on Ag-loaded TiO_2 nanotube arrays for photocatalytic CO_2 reduction. *Appl. Surf. Sci.* **2018**, *434*, 423–432. [CrossRef]
16. Reddy, B.V.N.; Reddy, B.V.S. Materials for Conversion of CO_2. *Biointerface Res. Appl. Chem.* **2021**, *12*, 486–497. [CrossRef]
17. Zhang, J.; Xu, J.; Tao, F. Interface Modification of TiO_2 Nanotubes by Biomass-Derived Carbon Quantum Dots for Enhanced Photocatalytic Reduction of CO_2. *ACS Appl. Energy Mater.* **2021**, *4*, 13120–13131. [CrossRef]
18. Celaya, C.A.; Méndez-Galván, M.; Castro-Ocampo, O.; Torres-Martínez, L.M.; Luévano-Hipólito, E.; Díaz de León, J.N.; Lara-García, H.A.; Díaz, G.; Muñiz, J. Exploring the CO_2 conversion into hydrocarbons via a photocatalytic process onto M-doped titanate nanotubes (M = Ni and Cu). *Fuel* **2022**, *324*, 124440. [CrossRef]
19. Kim, E.; Do, K.H.; Wang, J.; Hong, Y.; Putta Rangappa, A.; Amaranatha Reddy, D.; Praveen Kumar, D.; Kim, T.K. Construction of 1D TiO_2 nanotubes integrated ultrathin 2D ZnIn2S4 nanosheets heterostructure for highly efficient and selective photocatalytic CO_2 reduction. *Appl. Surf. Sci.* **2022**, *587*, 152895. [CrossRef]
20. Xiao, T.; Chen, Y.; Liang, Y. Visible light responsive metalloporphyrin-sensitized TiO_2 nanotube arrays for artificial photosynthesis of methane. *React. Chem. Eng.* **2022**, *7*, 917–928. [CrossRef]
21. Xiao, T.; Chen, Y.; Liang, Y. Ni(II) Tetra(4-carboxylphenyl)porphyrin-Sensitized TiO_2 Nanotube Array Composite for Efficient Photocatalytic Reduction of CO_2. *J. Phys. Chem. C* **2022**, *23*, 9742–9752. [CrossRef]
22. Ebhota, W.S.; Jen, T.C. Fossil Fuels Environmental Challenges and the Role of Solar Photovoltaic Technology Advances in Fast Tracking Hybrid Renewable Energy System. *Int. J. Precis. Eng. Manuf. Green Technol.* **2020**, *7*, 97–117. [CrossRef]
23. Raza Abbasi, K.; Fatai Adedoyin, F. Do energy use and economic policy uncertainty affect CO_2 emissions in China? Empirical evidence from the dynamic ARDL simulation approach. *Environ. Sci. Pollut. Res.* **2021**, *28*, 23323–23335. [CrossRef]
24. Wang, S.; Han, X.; Zhang, Y.; Tian, N.; Ma, T.; Huang, H. Inside-and-Out Semiconductor Engineering for CO_2 Photoreduction: From Recent Advances to New Trends. *Small Struct.* **2021**, *2*, 2000061. [CrossRef]
25. Behera, A.; Kar, A.K.; Srivastava, R. Challenges and prospects in the selective photoreduction of CO_2 to C1 and C2 products with nanostructured materials: A review. *Mater. Horizons* **2022**, *9*, 607–639. [CrossRef] [PubMed]
26. Ismael, M. Latest progress on the key operating parameters affecting the photocatalytic activity of TiO_2-based photocatalysts for hydrogen fuel production: A comprehensive review. *Fuel* **2021**, *303*, 121207. [CrossRef]
27. Wang, J.; Guo, R.T.; Bi, Z.X.; Chen, X.; Hu, X.; Pan, W.G. A review on TiO_2-x-based materials for photocatalytic CO_2 reduction. *Nanoscale* **2022**, *14*, 11512–11528. [CrossRef] [PubMed]
28. Shehzad, N.; Tahir, M.; Johari, K.; Murugesan, T.; Hussain, M. A critical review on TiO_2 based photocatalytic CO_2 reduction system: Strategies to improve efficiency. *J. CO2 Util.* **2018**, *26*, 98–122. [CrossRef]
29. Razzaq, A.; In, S.I. TiO_2 based nanostructures for photocatalytic CO_2 conversion to valuable chemicals. *Micromachines* **2019**, *10*, 326. [CrossRef] [PubMed]
30. Ismael, M. A review and recent advances in solar-to-hydrogen energy conversion based on photocatalytic water splitting over doped-TiO_2 nanoparticles. *Sol. Energy* **2020**, *211*, 522–546. [CrossRef]
31. Zhang, W.; He, H.; Li, H.; Duan, L.; Zu, L.; Zhai, Y.; Li, W.; Wang, L.; Fu, H.; Zhao, D. Visible-Light Responsive TiO_2-Based Materials for Efficient Solar Energy Utilization. *Adv. Energy Mater.* **2021**, *11*, 2003303. [CrossRef]
32. Hou, X.; Aitola, K.; Lund, P.D. TiO_2 nanotubes for dye-sensitized solar cells—A review. *Energy Sci. Eng.* **2020**, *9*, 921–937. [CrossRef]
33. Al Zoubi, W.; Salih Al-Hamdani, A.A.; Sunghun, B.; Ko, Y.G. A review on TiO_2-based composites for superior photocatalytic activity. *Rev. Inorg. Chem.* **2021**, *41*, 213–222. [CrossRef]

34. Tio, R.; Synthesis, N.M. Radial TiO_2 Nanorod-Based Mesocrystals: Synthesis, Characterization, and Applications. *Catalysts* **2021**, *11*, 1298.
35. Padmanabhan, N.T.; Thomas, N.; Louis, J.; Mathew, D.T.; Ganguly, P.; John, H.; Pillai, S.C. Graphene coupled TiO_2 photocatalysts for environmental applications: A review. *Chemosphere* **2021**, *271*, 129506. [CrossRef]
36. Anucha, C.B.; Altin, I.; Bacaksiz, E.; Stathopoulos, V.N. Titanium dioxide (TiO_2)-based photocatalyst materials activity enhancement for contaminants of emerging concern (CECs) degradation: In the light of modification strategies. *Chem. Eng. J. Adv.* **2022**, *10*, 100262. [CrossRef]
37. Suárez, S.; Jansson, I.; Ohtani, B.; Sánchez, B. From titania nanoparticles to decahedral anatase particles: Photocatalytic activity of TiO_2/zeolite hybrids for VOCs oxidation. *Catal. Today* **2019**, *326*, 2–7. [CrossRef]
38. Ismael, M. A review on graphitic carbon nitride (g-C3N4) based nanocomposites: Synthesis, categories, and their application in photocatalysis. *J. Alloys Compd.* **2020**, *846*, 156446. [CrossRef]
39. Reghunath, S.; Pinheiro, D.; KR, S.D. A review of hierarchical nanostructures of TiO_2: Advances and applications. *Appl. Surf. Sci. Adv.* **2021**, *3*, 100063. [CrossRef]
40. Shaikh, S.F.; Mane, R.S.; Min, B.K.; Hwang, Y.J.; Joo, O.S. D-sorbitol-induced phase control of TiO_2 nanoparticles and its application for dye-sensitized solar cells. *Sci. Rep.* **2016**, *6*, 20103. [CrossRef]
41. Wang, J.; Wang, X.; Chen, Q.; Xu, H.; Dai, M.; Zhang, M.; Wang, W.; Song, H. Microstructural modification of hollow TiO_2 nanospheres and their photocatalytic performance. *Appl. Surf. Sci.* **2021**, *535*, 147641. [CrossRef]
42. Chang, H.H.; Wei, L.W.; Huang, H.L.; Chang, H.Y.; Wang, H.P. Photocatalytic Reduction of CO_2 by TiO_2 Nanotubes. *Nano* **2022**, *17*, 2250032. [CrossRef]
43. Sun, L.; Zhang, S.; Sun, X.; He, X. Effect of the geometry of the anodized titania nanotube array on the performance of dye-sensitized solar cells. *J. Nanosci. Nanotechnol.* **2010**, *10*, 4551–4561. [CrossRef] [PubMed]
44. Kouao, D.S.; Grochowska, K.; Siuzdak, K. The Anodization of Thin Titania Layers as a Facile Process towards Semitransparent and Ordered Electrode Material. *Nanomaterials* **2022**, *12*, 1131. [CrossRef]
45. Lynch, R.P.; Ghicov, A.; Schmuki, P. A Photo-Electrochemical Investigation of Self-Organized TiO_2 Nanotubes. *J. Electrochem. Soc.* **2010**, *157*, G76. [CrossRef]
46. Tesler, A.B.; Altomare, M.; Schmuki, P. Morphology and Optical Properties of Highly Ordered TiO_2 Nanotubes Grown in NH4F/o-H_3PO_4 Electrolytes in View of Light-Harvesting and Catalytic Applications. *ACS Appl. Nano Mater.* **2020**, *3*, 10646–10658. [CrossRef]
47. Indira, K.; Mudali, U.K.; Nishimura, T.; Rajendran, N. A Review on TiO_2 Nanotubes: Influence of Anodization Parameters, Formation Mechanism, Properties, Corrosion Behavior, and Biomedical Applications. *J. Bio Tribo Corros.* **2015**, *1*, 28. [CrossRef]
48. Puga, M.L.; Venturini, J.; ten Caten, C.S.; Bergmann, C.P. Influencing parameters in the electrochemical anodization of TiO_2 nanotubes: Systematic review and meta-analysis. *Ceram. Int.* **2022**, *48*, 19513–19526. [CrossRef]
49. Bjelajac, A.; Petrović, R.; Vujancevic, J.; Veltruska, K.; Matolin, V.; Siketic, Z.; Provatas, G.; Jaksic, M.; Stan, G.E.; Socol, G.; et al. Sn-doped TiO_2 nanotubular thin film for photocatalytic degradation of methyl orange dye. *J. Phys. Chem. Solids* **2020**, *147*, 109609. [CrossRef]
50. Bjelajac, A.; Petrović, R.; Djokic, V.; Matolin, V.; Vondraček, M.; Dembele, K.; Moldovan, S.; Ersen, O.; Socol, G.; Mihailescu, I.N.; et al. Enhanced absorption of TiO_2 nanotubes by N-doping and CdS quantum dots sensitization: Insight into the structure. *RSC Adv.* **2018**, *8*, 35073–35082. [CrossRef]
51. Mahdi, N.; Kumar, P.; Goswami, A.; Perdicakis, B.; Shankar, K.; Sadrzadeh, M. Robust polymer nanocomposite membranes incorporating discrete TiO_2 nanotubes for water treatment. *Nanomaterials* **2019**, *9*, 1186. [CrossRef] [PubMed]
52. Wang, S.; Xu, M.; Peng, T.; Zhang, C.; Li, T.; Hussain, I.; Wang, J.; Tan, B. Porous hypercrosslinked polymer-TiO_2-graphene composite photocatalysts for visible-light-driven CO_2 conversion. *Nat. Commun.* **2019**, *10*, 676. [CrossRef] [PubMed]
53. Gao, J.; Qiu, G.; Li, H.; Li, M.; Li, C.; Qian, L.; Yang, B. Boron-doped graphene/TiO_2 nanotube-based aqueous lithium ion capacitors with high energy density. *Electrochim. Acta* **2020**, *329*, 135175. [CrossRef]
54. Yaashikaa, P.R.; Senthil Kumar, P.; Varjani, S.J.; Saravanan, A. A review on photochemical, biochemical and electrochemical transformation of CO_2 into value-added products. *J. CO2 Util.* **2019**, *33*, 131–147. [CrossRef]
55. Nguyen, T.P.; Nguyen, D.L.T.; Nguyen, V.H.; Le, T.H.; Vo, D.V.N.; Trinh, Q.T.; Bae, S.R.; Chae, S.Y.; Kim, S.Y.; Le, Q. Van Recent advances in TiO_2-based photocatalysts for reduction of CO_2 to fuels. *Nanomaterials* **2020**, *10*, 337. [CrossRef]
56. Fu, J.; Jiang, K.; Qiu, X.; Yu, J.; Liu, M. Product selectivity of photocatalytic CO_2 reduction reactions. *Mater. Today* **2020**, *32*, 222–243. [CrossRef]
57. Wang, J.; Lin, S.; Tian, N.; Ma, T.; Zhang, Y.; Huang, H. Nanostructured Metal Sulfides: Classification, Modification Strategy, and Solar-Driven CO_2 Reduction Application. *Adv. Funct. Mater.* **2021**, *31*, 2008008. [CrossRef]
58. Kang, X.; Liu, S.; Dai, Z.; He, Y.; Song, X.; Tan, Z. Titanium dioxide: From engineering to applications. *Catalysts* **2019**, *19*, 191. [CrossRef]
59. Savchuk, T.; Gavrilin, I.; Konstantinova, E. Anodic TiO_2 nanotube arrays for photocatalytic CO_2 conversion: Comparative photocatalysis and EPR study. *Nanotechnology* **2021**, *33*, 055706. [CrossRef]
60. Raskar, N.; Dake, D.; Khawal, H.; Deshpande, U.; Asokan, K.; Dole, B. Development of oxygen vacancies and surface defects in Mn-doped ZnO nanoflowers for enhancing visible light photocatalytic activity. *SN Appl. Sci.* **2020**, *2*, 1403. [CrossRef]

61. Zhang, J.; Li, J. The Oxygen Vacancy Defect of ZnO/NiO Nanomaterials Improves Photocatalytic Performance and Ammonia Sensing Performance. *Nanomaterials* **2022**, *12*, 433. [CrossRef] [PubMed]
62. Gao, J.; Shen, Q.; Guan, R.; Xue, J.; Liu, X.; Jia, H.; Li, Q.; Wu, Y. Oxygen vacancy self-doped black TiO_2 nanotube arrays by aluminothermic reduction for photocatalytic CO_2 reduction under visible light illumination. *J. CO2 Util.* **2020**, *35*, 205–215. [CrossRef]
63. Kar, P.; Zeng, S.; Zhang, Y.; Vahidzadeh, E.; Manuel, A.; Kisslinger, R.; Alam, K.M.; Thakur, U.K.; Mahdi, N.; Kumar, P.; et al. High rate CO_2 photoreduction using flame annealed TiO_2 nanotubes. *Appl. Catal. B Environ.* **2019**, *243*, 522–536. [CrossRef]
64. Zhang, Z.; Wang, Y.; Cui, G.; Lu, H.; Abanades, S. Remarkable CO_2 photoreduction activity using TiO_2 nanotube arrays under favorable photothermal conditions driven by concentrated solar light. *Appl. Phys. Lett.* **2021**, *119*, 123906. [CrossRef]
65. Santos, J.S.; Fereidooni, M.; Marquez, V.; Arumugam, M.; Tahir, M.; Praserthdam, S.; Praserthdam, P. Single-step fabrication of highly stable amorphous TiO_2 nanotubes arrays (am-TNTA) for stimulating gas-phase photoreduction of CO_2 to methane. *Chemosphere* **2022**, *289*, 133170. [CrossRef]
66. Pan, H.; Sun, M.; Wang, X.; Zhang, M.; Murugananthan, M.; Zhang, Y. A novel electric-assisted photocatalytic technique using self-doped TiO_2 nanotube films. *Appl. Catal. B Environ.* **2022**, *307*, 121174. [CrossRef]
67. Hu, X.; Xie, Z.; Tang, Q.; Wang, H.; Zhang, L.; Wang, J. Enhanced CH_4 yields by interfacial heating-induced hot water steam during photocatalytic CO_2 reduction. *Appl. Catal. B Environ.* **2021**, *298*, 120635. [CrossRef]
68. Sescu, A.M.; Favier, L.; Lutic, D.; Soto-Donoso, N.; Ciobanu, G.; Harja, M. TiO_2 doped with noble metals as an efficient solution for the photodegradation of hazardous organic water pollutants at ambient conditions. *Water* **2021**, *13*, 19. [CrossRef]
69. Juárez-Cortazar, D.E.; Torres-Torres, J.G.; Hernandez-Ramirez, A.; Arévalo-Pérez, J.C.; Cervantes-Uribe, A.; Godavarthi, S.; de los Monteros, A.E.E.; Silahua-Pavón, A.A.; Cordero-Garcia, A. Doping of TiO_2 Using Metal Waste (Door Key) to Improve Its Photocatalytic Efficiency in the Mineralization of an Emerging Contaminant in an Aqueous Environment. *Water* **2022**, *14*, 1389. [CrossRef]
70. Vargas Hernández, J.; Coste, S.; García Murillo, A.; Carrillo Romo, F.; Kassiba, A. Effects of metal doping (Cu, Ag, Eu) on the electronic and optical behavior of nanostructured TiO_2. *J. Alloys Compd.* **2017**, *710*, 355–363. [CrossRef]
71. Prakash, J.; Samriti; Kumar, A.; Dai, H.; Janegitz, B.C.; Krishnan, V.; Swart, H.C.; Sun, S. Novel rare earth metal–doped one-dimensional TiO_2 nanostructures: Fundamentals and multifunctional applications. *Mater. Today Sustain.* **2021**, *13*, 100066. [CrossRef]
72. Anucha, C.B.; Altin, I.; Bacaksız, E.; Kucukomeroglu, T.; Belay, M.H.; Stathopoulos, V.N. Enhanced photocatalytic activity of CuWO4 doped TiO_2 photocatalyst towards carbamazepine removal under UV irradiation. *Separations* **2021**, *8*, 25. [CrossRef]
73. Qian, X.; Yang, W.; Gao, S.; Xiao, J.; Basu, S.; Yoshimura, A.; Shi, Y.; Meunier, V.; Li, Q. Highly Selective, Defect-Induced Photocatalytic CO_2 Reduction to Acetaldehyde by the Nb-Doped TiO_2 Nanotube Array under Simulated Solar Illumination. *ACS Appl. Mater. Interfaces* **2020**, *12*, 55982–55993. [CrossRef] [PubMed]
74. Nguyen, N.H.; Wu, H.Y.; Bai, H. Photocatalytic reduction of NO_2 and CO_2 using molybdenum-doped titania nanotubes. *Chem. Eng. J.* **2015**, *269*, 60–66. [CrossRef]
75. Zhang, L.; Ren, Y.; Liu, W.; Wang, A.; Zhang, T. Single-atom catalyst: A rising star for green synthesis of fine chemicals. *Natl. Sci. Rev.* **2018**, *5*, 653–672. [CrossRef]
76. Hiragond, C.B.; Powar, N.S.; Lee, J.; In, S.I. Single-Atom Catalysts (SACs) for Photocatalytic CO_2 Reduction with H_2O: Activity, Product Selectivity, Stability, and Surface Chemistry. *Small* **2022**, *18*, 2201428. [CrossRef]
77. Pan, H.; Wang, X.; Xiong, Z.; Sun, M.; Murugananthan, M.; Zhang, Y. Enhanced photocatalytic CO_2 reduction with defective TiO_2 nanotubes modified by single-atom binary metal components. *Environ. Res.* **2021**, *198*, 111176. [CrossRef]
78. Gao, Y.; Qian, K.; Xu, B.; Li, Z.; Zheng, J.; Zhao, S.; Ding, F.; Sun, Y.; Xu, Z. Recent advances in visible-light-driven conversion of CO_2 by photocatalysts into fuels or value-added chemicals. *Carbon Resour. Convers.* **2020**, *3*, 46–59. [CrossRef]
79. Shinde, G.Y.; Mote, A.S.; Gawande, M.B. Recent Advances of Photocatalytic Hydrogenation of CO_2 to Methanol. *Catalysts* **2022**, *12*, 94. [CrossRef]
80. Vu, N.N.; Kaliaguine, S.; Do, T.O. Plasmonic Photocatalysts for Sunlight-Driven Reduction of CO_2: Details, Developments, and Perspectives. *ChemSusChem* **2020**, *13*, 3967–3991. [CrossRef]
81. Zhu, Q.; Xuan, Y.; Zhang, K.; Chang, K. Enhancing photocatalytic CO_2 reduction performance of g-C3N4-based catalysts with non-noble plasmonic nanoparticles. *Appl. Catal. B Environ.* **2021**, *297*, 120440. [CrossRef]
82. Ibrahim, N.S.; Leaw, W.L.; Mohamad, D.; Alias, S.H.; Nur, H. A critical review of metal-doped TiO_2 and its structure–physical properties–photocatalytic activity relationship in hydrogen production. *Int. J. Hydrogen Energy* **2020**, *45*, 28553–28565. [CrossRef]
83. Kar, P.; Farsinezhad, S.; Mahdi, N.; Zhang, Y.; Obuekwe, U.; Sharma, H.; Shen, J.; Semagina, N.; Shankar, K. Enhanced CH_4 yield by photocatalytic CO_2 reduction using TiO_2 nanotube arrays grafted with Au, Ru, and ZnPd nanoparticles. *Nano Res.* **2016**, *9*, 3478–3493. [CrossRef]
84. Khatun, F.; Abd Aziz, A.; Sim, L.C.; Monir, M.U. Plasmonic enhanced Au decorated TiO_2 nanotube arrays as a visible light active catalyst towards photocatalytic CO_2 conversion to CH_4. *J. Environ. Chem. Eng.* **2019**, *7*, 103233. [CrossRef]
85. Wang, Y.; Wang, Q.; Zhan, X.; Wang, F.; Safdar, M.; He, J. Visible light driven type II heterostructures and their enhanced photocatalysis properties: A review. *Nanoscale* **2013**, *5*, 8326–8339. [CrossRef]
86. Kavil, Y.N.; Shaban, Y.A.; Al Farawati, R.K.; Orif, M.I.; Zobidi, M.; Khan, S.U.M. Photocatalytic conversion of CO_2 into methanol over Cu-C/TiO_2 nanoparticles under UV light and natural sunlight. *J. Photochem. Photobiol. A Chem.* **2017**, *347*, 244–253. [CrossRef]

87. Li, Q.; Zong, L.; Li, C.; Yang, J. Photocatalytic reduction of CO_2 on MgO/TiO_2 nanotube films. *Appl. Surf. Sci.* **2014**, *314*, 458–463. [CrossRef]
88. Shi, Z.; Tan, Q.; Wu, D. Enhanced CO_2 hydrogenation to methanol over TiO_2 nanotubes-supported CuO-ZnO-CeO_2 catalyst. *Appl. Catal. A Gen.* **2019**, *581*, 58–66. [CrossRef]
89. De Almeida, J.; Pacheco, M.S.; de Brito, J.F.; de Arruda Rodrigues, C. Contribution of CuxO distribution, shape and ratio on TiO_2 nanotubes to improve methanol production from CO_2 photoelectroreduction. *J. Solid State Electrochem.* **2020**, *24*, 3013–3028. [CrossRef]
90. Goto, H.; Masegi, H.; Sadale, S.B.; Noda, K. Intricate behaviors of gas phase CO_2 photoreduction in high vacuum using Cu2O-loaded TiO_2 nanotube arrays. *J. CO2 Util.* **2022**, *59*, 101964. [CrossRef]
91. Bilgin Simsek, E. Solvothermal synthesized boron doped TiO_2 catalysts: Photocatalytic degradation of endocrine disrupting compounds and pharmaceuticals under visible light irradiation. *Appl. Catal. B Environ.* **2017**, *200*, 309–322. [CrossRef]
92. Kuo, C.Y.; Jheng, H.K.; Syu, S.E. Effect of non-metal doping on the photocatalytic activity of titanium dioxide on the photodegradation of aqueous bisphenol A. *Environ. Technol.* **2021**, *42*, 1603–1611. [CrossRef] [PubMed]
93. Delavari, S.; Amin, N.A.S.; Ghaedi, M. Photocatalytic conversion and kinetic study of CO_2 and CH_4 over nitrogen-doped titania nanotube arrays. *J. Clean. Prod.* **2016**, *111*, 143–154. [CrossRef]
94. Parayil, S.K.; Razzaq, A.; Park, S.M.; Kim, H.R.; Grimes, C.A.; In, S.I. Photocatalytic conversion of CO_2 to hydrocarbon fuel using carbon and nitrogen co-doped sodium titanate nanotubes. *Appl. Catal. A Gen.* **2015**, *498*, 205–213. [CrossRef]
95. Wang, Z.; Li, C.; Domen, K. Recent developments in heterogeneous photocatalysts for solar-driven overall water splitting. *Chem. Soc. Rev.* **2019**, *48*, 2109–2125. [CrossRef]
96. Rehman, Z.U.; Bilal, M.; Hou, J.; Butt, F.K.; Ahmad, J.; Ali, S.; Hussain, A. Photocatalytic CO_2 Reduction Using TiO_2-Based Photocatalysts and TiO_2 Z-Scheme Heterojunction Composites: A Review. *Molecules* **2022**, *27*, 2069. [CrossRef]
97. Wang, Y.; Zhu, C.; Zuo, G.; Guo, Y.; Xiao, W.; Dai, Y.; Kong, J.; Xu, X.; Zhou, Y.; Xie, A.; et al. 0D/2D Co_3O_4/TiO_2 Z-Scheme heterojunction for boosted photocatalytic degradation and mechanism investigation. *Appl. Catal. B Environ.* **2020**, *278*, 119298. [CrossRef]
98. Lai, Y.S.; Cheng, C.T.; Liou, J.L.; Jehng, J.M.; Dai, Y.M. The ZnO–Au-Titanium oxide nanotubes (TiNTs) composites photocatalysts for CO_2 reduction application. *Ceram. Int.* **2021**, *47*, 30020–30029. [CrossRef]
99. Wu, J.; Feng, Y.; Li, D.; Han, X.; Liu, J. Efficient photocatalytic CO_2 reduction by P–O linked g-C3N4/TiO_2-nanotubes Z-scheme composites. *Energy* **2019**, *178*, 168–175. [CrossRef]
100. Ikreedeegh, R.R.; Tahir, M. Photocatalytic CO_2 reduction to CO and CH_4 using g-C3N4/RGO on titania nanotube arrays (TNTAs). *J. Mater. Sci.* **2021**, *56*, 18989–19014. [CrossRef]
101. Li, X.; Liu, H.; Luo, D.; Li, J.; Huang, Y.; Li, H.; Fang, Y.; Xu, Y.; Zhu, L. Adsorption of CO_2 on heterostructure CdS(Bi 2S 3)/TiO_2 nanotube photocatalysts and their photocatalytic activities in the reduction of CO_2 to methanol under visible light irradiation. *Chem. Eng. J.* **2012**, *180*, 151–158. [CrossRef]
102. Cheng, M.; Bai, S.; Xia, Y.; Zhu, X.; Chen, R.; Liao, Q. Highly efficient photocatalytic conversion of gas phase CO_2 by TiO_2 nanotube array sensitized with CdS/ZnS quantum dots under visible light. *Int. J. Hydrogen Energy* **2021**, *46*, 31634–31646. [CrossRef]
103. Gonçalves, B.S.; Palhares, H.G.; Souza, T.C.C.D.; Castro, V.G.D.; Silva, G.G.; Silva, B.C.; Krambrock, K.; Soares, R.B.; Lins, V.F.C.; Houmard, M.; et al. Effect of the carbon loading on the structural and photocatalytic properties of reduced graphene oxide-TiO_2 nanocomposites prepared by hydrothermal synthesis. *J. Mater. Res. Technol.* **2019**, *8*, 6262–6274. [CrossRef]
104. Bian, J.; Huang, C.; Wang, L.; Daoud, W.A.; Zhang, R. C dots loading and TiO_2 nanorod length dependence of photoelectrochemical properties in C dots/TiO_2 nanorod array nanocomposites Supporting Information. *ACS Appl. Mater. Interfaces* **2014**, *6*, 4883–4890. [CrossRef]
105. Durga Devi, A.; Pushpavanam, S.; Singh, N.; Verma, J.; Kaur, M.P.; Roy, S.C. Enhanced methane yield by photoreduction of CO_2 at moderate temperature and pressure using Pt coated, graphene oxide wrapped TiO_2 nanotubes. *Results Eng.* **2022**, *14*, 100441. [CrossRef]
106. Dhabarde, N.; Selvaraj, J.; Yuda, A.; Kumar, A.; Subramanian, V.R. Review of photocatalytic and photo-electrocatalytic reduction of CO_2 on carbon supported films. *Int. J. Hydrogen Energy* **2022**, *47*, 30908–30936. [CrossRef]
107. Zubair, M.; Kim, H.; Razzaq, A.; Grimes, C.A.; In, S.I. Solar spectrum photocatalytic conversion of CO_2 to CH_4 utilizing TiO_2 nanotube arrays embedded with graphene quantum dots. *J. CO2 Util.* **2018**, *26*, 70–79. [CrossRef]
108. Sim, L.C.; Leong, K.H.; Saravanan, P.; Ibrahim, S. Rapid thermal reduced graphene oxide/Pt-TiO_2 nanotube arrays for enhanced visible-light-driven photocatalytic reduction of CO_2. *Appl. Surf. Sci.* **2015**, *358*, 122–129. [CrossRef]
109. Razzaq, A.; Grimes, C.A.; In, S. Il Facile fabrication of a noble metal-free photocatalyst: TiO_2 nanotube arrays covered with reduced graphene oxide. *Carbon N. Y.* **2016**, *98*, 537–544. [CrossRef]
110. Rambabu, Y.; Kumar, U.; Singhal, N.; Kaushal, M.; Jaiswal, M.; Jain, S.L.; Roy, S.C. Photocatalytic reduction of carbon dioxide using graphene oxide wrapped TiO_2 nanotubes. *Appl. Surf. Sci.* **2019**, *485*, 48–55. [CrossRef]
111. Thompson, W.A.; Sanchez Fernandez, E.; Maroto-Valer, M.M. Review and Analysis of CO_2 Photoreduction Kinetics. *ACS Sustain. Chem. Eng.* **2020**, *8*, 4677–4692. [CrossRef]

112. Ješić, D.; Lašič Jurković, D.; Pohar, A.; Suhadolnik, L.; Likozar, B. Engineering photocatalytic and photoelectrocatalytic CO_2 reduction reactions: Mechanisms, intrinsic kinetics, mass transfer resistances, reactors and multi-scale modelling simulations. *Chem. Eng. J.* **2021**, *407*, 126799. [CrossRef]
113. Liu, J.Y.; Gong, X.Q.; Alexandrova, A.N. Mechanism of CO_2 Photocatalytic Reduction to Methane and Methanol on Defected Anatase TiO_2 (101): A Density Functional Theory Study. *J. Phys. Chem. C* **2019**, *123*, 3505–3511. [CrossRef]
114. Núñez, O.; Sattayamuk, D.; Saelee, T.; Yamashita, H.; Kuwahara, Y.; Mori, K.; Praserthdam, P.; Praserthdam, S. A closer look inside TiO_2 (P25) photocatalytic CO_2/HCO_3- reduction with water. Methane rate and selectivity enhancements. *Chem. Eng. J.* **2021**, *409*, 128141. [CrossRef]
115. Khalilzadeh, A.; Shariati, A. Photoreduction of CO_2 over heterogeneous modified TiO_2 nanoparticles under visible light irradiation: Synthesis, process and kinetic study. *Sol. Energy* **2018**, *164*, 251–261. [CrossRef]
116. Lu, X.; Luo, X.; Thompson, W.A.; Tan, J.Z.Y.; Maroto-Valer, M.M. Investigation of carbon dioxide photoreduction process in a laboratory-scale photoreactor by computational fluid dynamic and reaction kinetic modeling. *Front. Chem. Sci. Eng.* **2021**, *16*, 1149–1163. [CrossRef]
117. Gong, E.; Ali, S.; Hiragond, C.B.; Kim, H.S.; Powar, N.S.; Kim, D.; Kim, H.; In, S.-I. Solar fuels: Research and development strategies to accelerate photocatalytic CO_2 conversion into hydrocarbon fuels. *Energy Environ. Sci.* **2022**, *15*, 880–937. [CrossRef]
118. Bjelajac, A.; Kopač, D.; Fecant, A.; Tavernier, E.; Petrović, R.; Likozar, B.; Janaćković, D. Micro-kinetic modelling of photocatalytic CO_2 reduction over undoped and N-doped TiO_2. *Catal. Sci. Technol.* **2020**, *10*, 1688–1698. [CrossRef]
119. Tan, L.L.; Ong, W.J.; Chai, S.P.; Mohamed, A.R. Photocatalytic reduction of CO_2 with H_2O over graphene oxide-supported oxygen-rich TiO_2 hybrid photocatalyst under visible light irradiation: Process and kinetic studies. *Chem. Eng. J.* **2017**, *308*, 248–255. [CrossRef]
120. Tahir, M.; Amin, N.S. Photocatalytic CO_2 reduction and kinetic study over In/TiO_2 nanoparticles supported microchannel monolith photoreactor. *Appl. Catal. A Gen.* **2013**, *467*, 483–496. [CrossRef]
121. Zhang, M.; Wang, M.; Xu, B.; Ma, D. How to Measure the Reaction Performance of Heterogeneous Catalytic Reactions Reliably. *Joule* **2019**, *3*, 2876–2883. [CrossRef]
122. Pineda, M.; Stamatakis, M. Kinetic Monte Carlo simulations for heterogeneous catalysis: Fundamentals, current status, and challenges. *J. Chem. Phys.* **2022**, *156*, 120902. [CrossRef] [PubMed]